Computer Physics Communications 184 (2013) 142–161

Contents lists available at SciVerse ScienceDirect

Computer Physics Communications

journal homepage: www.elsevier.com/locate/cpc

Self-consistent RPA calculations with Skyrme-type interactions: The skyrme_rpa program☆

Gianluca Colò [a,*], Ligang Cao [b,c,a], Nguyen Van Giai [d], Luigi Capelli [a,1]

[a] Dipartimento di Fisica, Università degli Studi, and INFN Sez. di Milano, via Celoria 16, 20133 Milano, Italy
[b] Institute of Modern Physics, Chinese Academy of Science, Lanzhou 730000, PR China
[c] Center of Theoretical Nuclear Physics, National Laboratory of Heavy Ion Accelerator of Lanzhou, Lanzhou 730000, PR China
[d] Institut de Physique Nucléaire, Univ. Paris-Sud and IN2P3-CNRS, F-91406 Orsay Cedex, France

ARTICLE INFO

Article history:
Received 18 September 2010
Received in revised form
25 July 2012
Accepted 30 July 2012
Available online 16 August 2012

Keywords:
Random Phase Approximation (RPA)
Hartree–Fock (HF)
Skyrme interaction

ABSTRACT

Random Phase Approximation (RPA) calculations are nowadays an indispensable tool in nuclear physics studies. We present here a complete version implemented with Skyrme-type interactions, with the spherical symmetry assumption, that can be used in cases where the effects of pairing correlations and of deformation can be ignored. The full self-consistency between the Hartree–Fock mean field and the RPA excitations is enforced, and it is numerically controlled by comparison with energy-weighted sum rules. The main limitations are that charge-exchange excitations and transitions involving spin operators are not included in this version.

Program summary

Program title: skyrme_rpa (v 1.00)
Catalogue identifier: AENF_v1_0
Program summary URL: http://cpc.cs.qub.ac.uk/summaries/AENF_v1_0.html
Program obtainable from: CPC Program Library, Queen's University, Belfast, N. Ireland
Licensing provisions: Standard CPC licence, http://cpc.cs.qub.ac.uk/licence/licence.html
No. of lines in distributed program, including test data, etc.: 5531
No. of bytes in distributed program, including test data, etc.: 39435
Distribution format: tar.gz
Programming language: FORTRAN-90/95; easily downgradable to FORTRAN-77.
Computer: PC with Intel Celeron, Intel Pentium, AMD Athlon and Intel Core Duo processors.
Operating system: Linux, Windows.
RAM: From 4 MBytes to 150 MBytes, depending on the size of the nucleus and of the model space for RPA.
Word size: The code is written with a prevalent use of double precision or
REAL(8) variables; this assures 15 significant digits.
Classification: 17.24.
Nature of problem: Systematic observations of excitation properties in finite nuclear systems can lead to improved knowledge of the nuclear matter equation of state as well as a better understanding of the effective interaction in the medium. This is the case of the nuclear giant resonances and low-lying collective excitations, which can be described as small amplitude collective motions in the framework of the Random Phase Approximation (RPA). This work provides a tool where one starts from an assumed form of nuclear effective interaction (the Skyrme forces) and builds the self-consistent Hartree–Fock mean field of a given nucleus, and then the RPA multipole excitations of that nucleus.
Solution method: The Hartree–Fock (HF) equations are solved in a radial mesh, using a Numerov algorithm. The solutions are iterated until self-consistency is achieved (in practice, when the energy

☆ This paper and its associated computer program are available via the Computer Physics Communication homepage on ScienceDirect (http://www.sciencedirect.com/science/journal/00104655).

* Corresponding author. Tel.: +39 02 50317241; fax: +39 02 50317487.
E-mail addresses: colo@mi.infn.it, gianluca.colo@mi.infn.it (G. Colò), caolg@impcas.ac.cn (L. Cao), nguyen@ipno.in2p3.fr (N. Van Giai), luigicapelli@futurainfonline.it (L. Capelli).
[1] Present address: Futura Informatica, via Botticelli 3a, 20020 Villa Cortese (MI), Italy.

0010-4655/$ – see front matter
doi:10.1016/j.cpc.2012.07.016

eigenvalues are stable within a desired accuracy). In the obtained mean field, unoccupied states necessary for the RPA calculations are found. For all single-particle states, box boundary conditions are assumed. To solve the RPA problem for a given value of total angular momentum and parity J^π a coupled basis is constructed and the RPA matrix is diagonalized (protons and neutrons are treated explicitly, and no approximation related to the use of isospin formalism is introduced). The transition amplitudes and transition strengths associated to given external operators are calculated. The HF densities and RPA transition densities are also evaluated.

Restrictions: The main restrictions are related to the assumed spherical symmetry and absence of pairing correlations.

Running time: The typical running time depends strongly on the nucleus, on the multipolarity, on the choice of the model space and of course on the computer. It can vary from a few minutes to several hours.

1. Introduction

Atomic nuclei have a very rich variety of excitation spectra ranging from elementary excitations of single-particle nature to completely collective modes like rotational motion where the entire nucleus participates as a whole. The vibrational collective modes constitute a typical example of coherent behavior where the excited states are built out of a constructive superposition of elementary excitations, which results in a state largely shifted from the energy region of the elementary excitations, with a considerably increased strength. Well-known examples are the low-lying vibrations and the high-lying giant resonances which are the objects of many theoretical and experimental investigations [1].

There is now a well-established microscopic framework which allows one to understand, and also to predict to a certain extent, many of these nuclear properties. The generally accepted approach is the Energy Density Functional framework which allows one to construct the self-consistent nuclear mean field. The Skyrme effective interaction is one of the earliest energy functionals [2] and it remains the most widely used.

The Skyrme-type interactions were originally designed for describing the static Hartree–Fock (HF) mean field, and their parameters are generally determined by adjusting selected bulk properties of infinite matter and ground states of finite nuclei. It turned out that they can give also a relevant description of nuclear excitations through the Random Phase Approximation (RPA) which is the well-known small amplitude limit of the time-dependent Hartree–Fock (TDHF) approximation and was exploited already in the early 1970s. RPA coupled equations allow treating the continuum exactly, and they have been solved using Skyrme forces in Ref. [3]. Green's function RPA has been formulated with Skyrme forces, with or without [4,5] the continuum; the first self-consistent continuum calculations were presented in Ref. [6]. No fully self-consistent calculations exist, however, within the Green's function framework. Fully self-consistent versions of RPA have been developed employing the matrix formulation of RPA, first in Refs. [7,8]. The code explained in this paper is of the same kind and its first results were discussed in Ref. [9]. Nowadays there are many applications with many more refinements: spherical symmetry or deformations, finite temperature, pairing correlation effects, etc. A new method to solve RPA, the so-called finite amplitude method, has been recently introduced [10].

The purpose of this paper is to present to a wide audience in the nuclear physics community — theorists and experimentalists — a tool which allows one to compute a wide variety of nuclear excitations in the framework of HF-RPA. This HF-RPA code is fully self-consistent. It can be used with practically all existing parameterizations of Skyrme-type interactions, except those with two-body tensor interactions or with velocity-and-density dependent terms. The main limitations are: (1) a spherical symmetry assumption; (2) zero temperature; (3) pairing correlations are not present; (4) the nucleus under study must have filled subshells, i.e., partial occupancies are not included; (5) the unnatural parity states having $\pi = (-1)^{J\pm1}$ and, more generally, transitions induced by operators involving spin operators are not treated in the present version; (6) the continuum is discretized. Concerning this latter point we remind the reader that there are no serious discrepancies between discrete and continuum RPA as far as peak or centroid energies of collective states are concerned, except for weakly bound nuclei. A recent study within the relativistic mean field framework can be found in Ref. [11], and it has reached similar conclusions.

The numerical code contains two parts which are linked together. The first part is the HF code which carries out the Hartree–Fock computations of a specified (N, Z) nucleus using an interaction contained in a list: this list is in an external file (see Section 3.2) and users can modify it according to their needs. The resulting HF mean fields and densities serve as inputs to the second part which constitutes the RPA code.

This article is organized as follows. In Section 2 we summarize the main formalism used in the HF and RPA codes. Section 2.1 is devoted to the HF part, and Section 2.2 to the RPA part. In Section 3 we explain the inputs of the code and we comment on their choice. A short conclusion is given in Section 4. In Appendices A–C are examples of input and output of a typical calculation.

2. Formalism

In this section we give the main indications which are needed to understand the structure of the calculations leading to the final RPA results. There are two parts in the computations which must be carried out sequentially. In the first part, described in Section 2.1, one determines self-consistently the Hartree–Fock mean field by an iterative procedure which is repeated until convergence. In the second part, described in Section 2.2, the RPA matrix is built and then diagonalized. The output information includes not only the RPA eigenvalues, but also the transition amplitudes and strengths associated with each state, as well as the corresponding sum rules: these quantities are discussed in Section 2.3, together with the appropriate external operators.

2.1. Hartree–Fock mean field and single-particle states

We adopt the notation of Ref. [12] (at the same time, we recall that the earlier HF calculations for spherical nuclei have been published in Refs. [2,13], where many useful details can be found). The two nucleons with space, spin and isospin variables $\mathbf{r}_i$, $\boldsymbol{\sigma}_i$, $\boldsymbol{\tau}_i$ are interacting

through a zero-range, velocity-dependent Skyrme interaction written in a standard form:

$$V(\mathbf{r}_1,\mathbf{r}_2) = t_0(1+x_0P_\sigma)\delta(\mathbf{r}) + \frac{1}{2}t_1(1+x_1P_\sigma)[\mathbf{P}'^2\delta(\mathbf{r}) + \delta(\mathbf{r})\mathbf{P}^2] + t_2(1+x_2P_\sigma)\mathbf{P}'\cdot\delta(\mathbf{r})\mathbf{P} + \frac{1}{6}t_3(1+x_3P_\sigma)\rho^\alpha(\mathbf{R})\delta(\mathbf{r}) + iW_0(\boldsymbol{\sigma}_1+\boldsymbol{\sigma}_2)\cdot[\mathbf{P}'\times\delta(\mathbf{r})\mathbf{P}], \quad (1)$$

where $\mathbf{r}=\mathbf{r}_1-\mathbf{r}_2$, $\mathbf{R}=\frac{1}{2}(\mathbf{r}_1+\mathbf{r}_2)$, $\mathbf{P}=\frac{1}{2i}(\nabla_1-\nabla_2)$, $\mathbf{P}'$ is the hermitian conjugate of $\mathbf{P}$ (acting on the left), and $P_\sigma=\frac{1}{2}(1+\boldsymbol{\sigma}_1\cdot\boldsymbol{\sigma}_2)$ is the spin-exchange operator. Here, $\rho=\rho_n+\rho_p$ is the total nucleon density, and we will use the notation ρ_q to distinguish the neutron ($q=0$) and proton ($q=1$) densities. Note that the isospin-exchange operator does not explicitly appear because it can always be expressed in terms of P_σ due to the zero-range nature of the Skyrme force.

In the original form given by Skyrme [14,15] there was no explicit density-dependent term but a three-body contact term with a strength parameter t_3. In the HF approximation the contribution of this three-body contact term is the same as that given by the t_3 term of Eq. (1) when $x_3=1$ and $\alpha=1$. The density dependence of the force is very important for a satisfactory description of nuclear density profiles, and the parameterization (1) gives more flexibility for adjusting the compression modulus of nuclear matter and the energy of the giant monopole resonance in nuclei. Besides the standard form (1) there are also attempts to introduce various variants of the density-dependent term such as $\frac{1}{6}t_3(1+x_3P_\sigma)(\rho_q+\rho_{q'})^\alpha\delta(\mathbf{r})$ or $\frac{1}{2}t_4(1+x_4P_\sigma)\left[\mathbf{P}'^2(\rho_q+\rho_{q'})^\beta\delta(\mathbf{r})+h.c.\right]$, where q and q' stand for neutron or proton. These variants are not treated in the present computer code.

The procedure for deriving the Skyrme–Hartree–Fock equations has been described in various papers, and for instance we refer the reader to Ref. [12] for the spherical symmetry case which we consider here. The starting point is the assumption that the ground state wave function is a Slater determinant built on the single-particle (s.p.) wave functions of the *occupied* orbitals $\varphi^q_\alpha(\mathbf{r})$. The total energy must be stationary under norm-conserving variations of the $\{\varphi^q_\alpha(\mathbf{r})\}$:

$$\delta\left(E-\sum_\alpha\epsilon_\alpha\int|\varphi^q_\alpha(\mathbf{r})|^2d^3r\right)=0. \quad (2)$$

This stationarity condition leads to the Skyrme–HF equations:

$$\left[-\nabla\cdot\frac{\hbar^2}{2m^*_q(\mathbf{r})}\nabla+U_q(\mathbf{r})+qV_C(\mathbf{r})-i\mathbf{W}_q(\mathbf{r})\cdot(\nabla\times\boldsymbol{\sigma})\right]\varphi^q_\alpha=\epsilon_\alpha\varphi^q_\alpha, \quad (3)$$

where the index α refers to occupied states. These equations, although highly non-linear because of the self-consistency problem, involve only local potentials, and therefore they may be solved in coordinate space. This is a major difference with HF equations corresponding to finite range interactions which give rise to fully non-local potentials and one has generally to use a discrete basis (e.g., a harmonic oscillator basis) to find the solutions. A discrete basis (made up with harmonic oscillator or Woods–Saxon wave functions with box boundary conditions) could in principle be used also for Skyrme–HF equations. For well-bound states this does not make any difference. Recently, many authors have addressed the problem of the inadequacies of some basis expansions in the case of weakly bound states. We do not discuss these issues here.

Note that the eigenvalues ϵ_α are just the Lagrange multipliers introduced in Eq. (2). They are often called for convenience s.p. energies. In the above Skyrme–HF equation, the effective masses m^*_q, central potentials U_q and spin–orbit potentials $\mathbf{W}_q$ can be expressed in terms of the *local* s.p. densities ρ_q and their derivatives, the kinetic energy densities τ_q and the so-called spin–orbit densities $\mathbf{J_q}$. This means that they are known when all the *occupied* states are known. This is where the self-consistency of the approach resides. We note also that the same Eqs. (3) can determine not only the occupied states but also the unoccupied states once convergence is reached, i.e., the complete set of particle–hole (p–h) states needed to build the RPA is obtained from Eqs. (3).

In the past, some Skyrme parameter sets have been fitted and used without including, at the mean field level, the terms which depend on the spin–orbit densities $\mathbf{J_q}$. These terms are called for simplicity, in the literature and here, "$\mathbf{J^2}$ terms". Accordingly, these terms are automatically included or dropped in HF with the present values of the flag in the last line of the file SKYRME.IN (see Table 1 in Section 3.1). The corresponding terms of the residual p–h interaction are also automatically included or dropped in RPA. In such a way, this RPA code always preserves the full self-consistency. We have checked that, as a rule, the $\mathbf{J^2}$ terms produce a small effect on the natural-parity excitations that can be studied with the present code. On the other hand, in the case of spin excitations, the effect of the $\mathbf{J^2}$ terms in the residual interaction is larger. It should be kept in mind that these $\mathbf{J^2}$ terms of the residual interaction are not usually well constrained when the fit of the force parameters is performed, as only quantities that are rather insensitive to the $\mathbf{J^2}$ terms (like the binding energies of doubly magic nuclei) are considered. For a more detailed discussion, the reader can consult [16] (and the references therein).

The Coulomb potential requires an additional approximation for the exchange contribution in order to keep it local in Eq. (3) (the Coulomb interaction, unlike the Skyrme force, has a non-zero range). A local density approximation called the Slater approximation [17] is used for expressing the Coulomb exchange contribution to the total energy:

$$E^{ex}_C=-\frac{3e^2}{4}\left(\frac{3}{\pi}\right)^{\frac{1}{3}}\int\rho_p^{\frac{4}{3}}d^3r. \quad (4)$$

This expression gives the exact result in infinite matter. With this approximation the one-body Coulomb potential becomes

$$V_C(\mathbf{r})=\frac{e^2}{2}\left[\int\frac{\rho_p(\mathbf{r}')}{|\mathbf{r}-\mathbf{r}'|}d^3r'-\left[\frac{3}{\pi}\rho_p(\mathbf{r})\right]^{\frac{1}{3}}\right]. \quad (5)$$

The accuracy of the Slater approximation in finite nuclei has been checked in Ref. [18], and found to be rather good. It has to be noted that some authors define the Coulomb potential by using the charge density, whereas most Skyrme interactions have been fitted by considering the point-proton density, and this approach is adopted also in the present computer code.

Table 1
A typical Skyrme parameter set in the format which should be used in the file `skyrme.in`.

File text	Comment
//SLy5: NPA 643 (1998) 441	Comment line (the code will ignore it)
[SLy5]	Name of the parameter set
−2484.88d0	t_0
483.13d0	t_1
−549.40d0	t_2
13763.d0	t_3
0.778d0	x_0
−0.328d0	x_1
−1.d0	x_2
1.267d0	x_3
126.d0	W_0
126.d0	W_0'
0.1666666d0	α
1	Flag set at 0 (1) if the force was fitted without (with) the J^2 terms

The full treatment of the center-of-mass correction to the total energy is another source of complication which would hurt the simplicity of the Skyrme–HF approach. Indeed, the kinetic energy part of the total energy E is not exactly $\sum_i^A \mathbf{p}_i^2/2m$ because the kinetic energy of the center of mass must be subtracted:

$$\begin{aligned} T &= \sum_i^A \frac{\mathbf{p}_i^2}{2m} - \frac{\left(\sum_i^A \mathbf{p}_i\right)^2}{2mA} \\ &= \frac{1}{2m}\left(1-\frac{1}{A}\right)\sum_i^A \mathbf{p}_i^2 - \frac{1}{2mA}\sum_{i\neq j}^A \mathbf{p}_i\cdot\mathbf{p}_j. \end{aligned} \tag{6}$$

The first term on the second line is again a one-body kinetic term with a corrected mass $m' = m\frac{A}{A-1}$. This takes care of a large part of the center-of-mass correction on the total energy, and it is included in practically all Skyrme–HF calculations. As we shall explain at the end of Section 2.3, this term affects the value of the so-called energy-weighted sum rules associated with the RPA results. The second term is a two-body correction that is much more difficult to incorporate and it is usually dropped in constructing Skyrme forces and their subsequent applications. This does not mean that this term is small but simply that the forces have been adjusted without it.

In the case of spherical symmetry the three-dimensional HF equations (3) simplify greatly into a set of one-dimensional differential equations in the radial coordinate r. The s.p. index α now stands for the set of quantum numbers $\{\epsilon_\alpha, l, j, m\}$, and the s.p. wave functions can be factorized into

$$\varphi_\alpha^q(\mathbf{r},\sigma) = \frac{u_\alpha^q(r)}{r}[Y_l(\hat{r})\otimes\chi_{1/2}(\sigma)]_{jm}\chi_q(\tau), \tag{7}$$

where χ is a two-component (iso-)spinor. We shall often omit writing the isospin index q of the s.p. wave function explicitly, unless necessary. The HF Slater determinant is assumed time-reversal invariant and all potentials appearing in the HF equations (3) are spherically symmetric. One can easily deduce the HF radial equations:

$$\frac{\hbar^2}{2m_q^*(r)}\left[-u_\alpha'' + \frac{l(l+1)}{r^2}u_\alpha\right] + V_q(r)u_\alpha - \left(\frac{\hbar^2}{2m_q^*}\right)' u_\alpha' = \epsilon_\alpha u_\alpha, \tag{8}$$

where the HF potential is a sum of central, Coulomb and spin–orbit terms:

$$V_q(r) = V_q^{cent}(r) + \delta_{q,1}V_C(r) + V_q^{s.o.}(r)\langle\mathbf{l}\cdot\sigma\rangle. \tag{9}$$

The radial HF equations can be easily solved numerically by using a Numerov algorithm.

Thus, the procedure to construct all necessary single-particle states before starting a given RPA calculation is as follows.

1. Start with an ensemble of trial wave functions $\{u_\alpha, \alpha = 1, 2, \ldots, N\}$ for the occupied states (in the present case, they are eigenfunctions of a standard Woods–Saxon potential).
2. Construct the potentials $V_q(r)$ and effective masses $m_q^*(r)$.
3. Solve Eqs. (3) for a new set of $\{u_\alpha, \alpha = 1, 2, \ldots, N\}$.
4. Repeat steps 2–3 until convergence.
5. Calculate with the converged potentials and effective masses all wave functions $\{u_\alpha, \alpha = N+1, N+2, \ldots\}$ of unoccupied states necessary for the RPA calculation. All single-particle states (occupied and unoccupied) are calculated using a box boundary condition.

2.2. RPA equations

Under the spherical symmetry assumption the RPA excited states have good angular momentum and parity J^π, and therefore each J^π-mode corresponds to a separate RPA diagonalization in the corresponding J^π particle–hole space. The RPA method is well known from textbooks [19]. Below, we shall only recall the main steps in order to indicate our notation and phase conventions, which mainly follow those of [20].

We denote by $\alpha = \{n_a, l_a, j_a, q_a, m_a\} = \{a, m_a\}$ a general single-particle state with principal quantum number n_a, orbital and total angular momenta l_a, j_a, charge index q_a and total angular momentum projection m_a. The corresponding creation and annihilation operators are c^+_α and c_α. Occupied (unoccupied) states will be denoted by $a = i, j, \ldots$ $(a = m, n, \ldots)$. The creation operator of a particle–hole (p–h) pair coupled to total angular momentum (JM) is

$$Q^+_{mi}(JM) = \sum_{m_m, m_i} (j_m j_i m_m - m_i | JM) c^+_{j_m m_m} (-1)^{j_i - m_i} c_{j_i m_i}, \tag{10}$$

where both m and i states have the same charge index. In RPA, the excited states $|\nu\rangle$ result from the action of excitation operators O^+_ν on the correlated RPA ground state denoted by $|\tilde{0}\rangle$:

$$|\nu\rangle = O^+_\nu |\tilde{0}\rangle, \tag{11}$$

and these RPA operators can be expressed in terms of the Q^+ and Q operators like in Ref. [20], namely

$$O^+_\nu = \sum_{mi} X^{(\nu)}_{mi} Q^+_{mi}(JM) - Y^{(\nu)}_{mi} Q_{mi}(\widetilde{JM}), \tag{12}$$

where the symbol $\widetilde{JM}$ denotes the time-reversed state of JM. With the additional assumption that the correlated RPA ground state is the vacuum for the RPA operators O_ν one can show that the X^ν, Y^ν amplitudes are the eigenvectors of the RPA secular matrix:

$$\begin{pmatrix} A & B \\ -B & -A \end{pmatrix} \begin{pmatrix} X^{(\nu)} \\ Y^{(\nu)} \end{pmatrix} = E_\nu \begin{pmatrix} X^{(\nu)} \\ Y^{(\nu)} \end{pmatrix}, \tag{13}$$

and the corresponding eigenvalues are the excitation energies of the RPA modes. If the dimension of the p–h configuration space is N, the matrices A and B are $N \times N$ symmetric matrices whose expressions are

$$A_{mi,nj} = (\epsilon_m - \epsilon_i)\, \delta_{mn}\delta_{ij} + \langle \overbrace{m\underbrace{j|V_{res}|i}_{J}\, n}^{J} \rangle, \tag{14}$$

$$B_{mi,nj} = \langle \overbrace{mn|V_{res}|\underbrace{i\, j}_{J}}^{J} \rangle. \tag{15}$$

In these formulas the p–h coupled matrix elements of the residual interaction V_{res} appear. They are defined as

$$\langle \overbrace{\underbrace{ab|V_{res}|c}_{J}\, d}^{J} \rangle = \sum_{\text{all } m} (-)^{j_b - m_b + j_c - m_c} (j_a j_c m_a - m_c | JM)(j_d j_b m_d - m_b | JM) \langle j_a m_a, j_b m_b | V_{res} | j_c m_c, j_d m_d \rangle. \tag{16}$$

The user of the present code should be aware that in all the RPA part the phase convention of the single-particle wave functions differs from that of Eq. (7) by the phase factor i^l. Also, we should state clearly that our RPA formalism, while employing a coupled scheme in the total angular momentum J, is not isospin coupled. Rather, it treats neutrons and protons explicitly. The present code deals only with non-charge-exchange excitations: the p–h pairs are made up with nucleons having the same charge, and we will denote by q and q' the charge states of the two pairs mi and nj. Accordingly, the residual interaction will be labelled by $V^{qq'}_{res}$.

This residual interaction is simply the antisymmetrized particle–hole interaction, i.e., $V\,(1 - P_{12})$, where P_{12} is the operator exchanging particles 1 and 2, if the starting interaction V has no density dependence. Since the Skyrme interaction given by Eq. (1) depends actually on density, one must use instead the more general expression

$$V^{qq'}_{res} = \frac{\delta^2 E}{\delta \rho_q \delta \rho_{q'}}, \tag{17}$$

where E is the HF energy functional (see, e.g., Section 3 of Ref. [4]). For the terms t_0, t_1, t_2 and for the spin–orbit term W_0, the expressions provided by Eq. (17) coincide with the $V(1 - P_{12})$ form. This is not the case for the term t_3: due to the explicit density dependence the result of (17) differs from the $V(1 - P_{12})$ interaction corresponding to t_3 and the terms associated with this difference are usually called "rearrangement terms" in the literature. For the sake of completeness, we provide explicit formulas in Appendix A. We also mention the particle–hole interaction due to the Coulomb term: for consistency with the HF treatment, its direct term is taken into account exactly whereas its exchange term results from Eq. (17) applied to the Slater approximation of the exchange Coulomb energy. In summary, Eq. (17) is used systematically and this allows for the fulfilment of the proper conservation laws (as testified, for example, from sum rules and the position of the spurious state). We shall discuss below the corresponding numerical results.

In practice, the procedure, which starts from the HF output and is aimed at obtaining the complete information about the vibrational states, is as follows.

1. Given a J^π value, construct an N-dimensional basis of coupled p–h configurations $\{mi\}$ associated with the Q^+_{mi} operators of Eq. (10). For this, all possible occupied states i are considered together with all possible unoccupied states m lying below a cutoff energy E_C.
2. Build the matrix elements defined by Eqs. (14) and (15).
3. Diagonalize the RPA matrix (13). The effort of diagonalizing the $2N \times 2N$ matrix is reduced by means of the algorithm introduced by [21].
4. Calculate the quantities of interest associated with the states labelled by ν in (13): transition amplitudes associated with a given operator $\hat{F}$, transition strengths and transition densities. These quantities deserve a specific discussion in the next subsection.

We end the present subsection by a remark about the possible values of J^π. In principle, the present code can build the RPA matrix and diagonalize it for any values of spin and parity. However, it is intended to be used for natural parity states $\pi = (-1)^J$ in connection with spin-independent operators (see below). The extension to the spin-dependent case is not difficult but it is not contained in the present version.

2.3. Transition amplitudes and strengths, sum rules and transition densities

Once the RPA equations are solved for a given J^π, one has the complete set of eigenvalues and eigenvectors for all vibrational states ν. The vibrational states are excited under the action of an external field, which can be electromagnetic or hadronic. Let us first introduce general isoscalar and isovector external fields and recall their related sum rule properties. The J-multipole of an isoscalar (respectively, isovector) external field is defined by its component $\hat{F}^{IS}_J$ (respectively, $\hat{F}^{IV}_J$):

$$\hat{F}^{(IS)}_J = \sum_{i=1}^{A} f_J(r_i) Y_{JM}(\hat{r}_i),$$
$$\hat{F}^{(IV)}_J = \sum_{i=1}^{A} f_J(r_i) Y_{JM}(\hat{r}_i)\tau_z(i), \tag{18}$$

where the sums run over all nucleons and $\tau_z(i)$ is the z-component of the isospin operator of nucleon i. The function $f_J(r)$ is arbitrary; it often corresponds to a spherical Bessel function for electromagnetic external fields or it becomes proportional to r^J in the long wavelength limit.

The electromagnetic excitation process, using either real photons or virtual photons (Coulomb excitation), is treated in textbooks. The multipole decomposition of the photon plane wave leads to terms which contain Bessel functions $j_J(qr)$, where q is the photon momentum. In cases of interest, where the excitation energy is of the order of $\approx$10 MeV and r can be about the size of the nuclear radius, the long wavelength limit ($qr \ll 1$) of the Bessel functions can be used, and the excitation operator becomes proportional to

$$\hat{F}_{JM} = e \sum_{i=1}^{A} r_i^J Y_{JM}(\hat{r}_i) \frac{1}{2}(1 - \tau_z(i)). \tag{19}$$

In the dipole case, it is customary to remove the contribution from the center of mass, so that the electromagnetic operator becomes

$$\hat{F}_{1M} = \frac{eN}{A} \sum_{i=1}^{Z} r_i Y_{1M}(\hat{r}_i) - \frac{eZ}{A} \sum_{i=1}^{N} r_i Y_{1M}(\hat{r}_i); \tag{20}$$

that is, the effective charge for protons (neutrons) turns out to be $\frac{eN}{A}$ $\left(-\frac{eZ}{A}\right)$. In principle, this subtraction should be done for every multipole. However, for $L \geq 2$ the resulting effective charges do not differ significantly from 1 and 0 for heavy nuclei (see their expression, e.g., on p. 98 of Ref. [22]): as a consequence, we do not correct the form (19) for cases other than the dipole.

In the case of hadron inelastic scattering, one arrives at similar excitation operators starting, for example, from the Distorted Wave Born Approximation (DWBA) expression for the cross section. This cross section is in fact proportional to the square of the transition amplitude [1]

$$T_{fi} = \int d^3\mathbf{R}\, \chi_f^*(\mathbf{R}) \langle f|V(\mathbf{R})|i\rangle \chi_i(\mathbf{R}), \tag{21}$$

where χ stands for the distorted waves describing the relative projectile–target motion, $\mathbf{R}$ is the distance between the corresponding centers of mass, and V is the projectile–target interaction. One should note that the previous equation is not the most general one. If the interaction V has finite range, the formula holds only if the exchange part of the transition amplitude is either neglected or approximated so that it can be written as local (for instance, by using a Slater approximation). However, we would only like to point out here the following feature. Under the assumptions of (i) distorted waves replaced by plane waves, (ii) zero-range interaction of the form $V_0 \sum_i^A \delta(\mathbf{r_i} - \mathbf{R}) + V_1 \sum_i^A \delta(\mathbf{r_i} - \mathbf{R})\boldsymbol{\tau}(i) \cdot \mathbf{T}$, where $\mathbf{T}$ is the projectile isospin, and (iii) small momentum transfer $\mathbf{q}$, the DWBA transition amplitude T_{fi} for non-charge-changing transitions becomes clearly proportional to the matrix elements of the fields $\hat{F}^{(IS)}_{JM}$ and $\hat{F}^{(IV)}_{JM}$ of Eq. (18) with $f_J(r) = r^J$.

The (reduced) transition strength is generally given by

$$B(EJ, i \to f) = \frac{1}{2J_i + 1} |\langle f||\hat{F}_J||i\rangle|^2, \tag{22}$$

where $\langle f||\hat{F}_J||i\rangle$ is the reduced matrix element of $\hat{F}_{JM}$ (see, e.g., Ref. [23]). In the present case the initial state is the RPA ground state with zero angular momentum. For the final states ν described in the previous subsection, the formula becomes

$$B(EJ, \tilde{0} \to \nu) = \left| \sum_{mi} \left(X^{(\nu)}_{mi} + Y^{(\nu)}_{mi} \right) \langle m||\hat{F}_J||i\rangle \right|^2 ; \tag{23}$$

i.e., the transition strength is the square of the so-called transition amplitude and the latter can be large if many p–h configurations $\{mi\}$ do contribute coherently in the sum.

The strength function is defined as

$$S(E) = \sum_\nu |\langle \nu||\hat{F}_J||\tilde{0}\rangle|^2 \delta(E - E_\nu), \tag{24}$$

and it consists, within this configuration space RPA, of a sum of delta functions. Its moments

$$m_k = \int dE\, E^k S(E) = \sum_\nu |\langle \nu||\hat{F}_J||\tilde{0}\rangle|^2 E_\nu^k \tag{25}$$

are calculated by the present code and will be discussed below.

Among them the linear moment m_1 (energy-weighted sum rule, or EWSR) is an object of consideration since, due to the Thouless theorem [24], its value equals one half of the HF expectation value of the double commutator $\left[\hat{F}, \left[H, \hat{F}\right]\right]$.

We give here the general expressions [8] corresponding to the operators (18). For isoscalar operators, only the kinetic part of the Skyrme Hamiltonian contributes, and one has

$$m_1^{(IS)}(J) = \frac{\hbar^2}{2m}\frac{A}{4\pi}(2J+1)\langle g_J\rangle, \tag{26}$$

where

$$\langle g_J\rangle = \frac{1}{A}\int g_J(r)\rho(r)d^3r,$$

$$g_J(r) = \left(\frac{df_J}{dr}\right)^2 + J(J+1)\left(\frac{f_J}{r}\right)^2. \tag{27}$$

For isovector operators, the velocity-dependent terms of the Skyrme interaction contribute to the enhancement factor $\tilde{\kappa}$, and one has

$$m_1^{(IV)}(J) = m_1^{(IS)}(J)(1+\tilde{\kappa}), \tag{28}$$

where $\tilde{\kappa}$ is

$$\tilde{\kappa} = \frac{2m/\hbar^2}{A\langle g_J\rangle}\left(t_1\left(1+\frac{x_1}{2}\right) + t_2\left(1+\frac{x_2}{2}\right)\right)\int g_J(r)\rho_n(r)\rho_p(r)d^3r. \tag{29}$$

In all cases, the result of Eqs. (26) and (28) should be recovered by the numerical solution of the RPA equations. Accordingly, the present code provides this result under the label ‘‘M(1) D.C’’. (where D.C. stands for “double commutator”), as well as the percentage exhausted in the numerical calculation at hand, in the case of $J \geq 2$.

Let us now review some important cases. In the $J = 0$ case non-vanishing excitations are produced by the next term in the expansion of the Bessel function $j_0(qr)$, that is, if the operator

$$\hat{F}^{(\text{IS monopole})} = \sum_{i=1}^{A} r_i^2 Y_{00} \tag{30}$$

is considered. The associated double commutator sum rule is

$$m_1 = \frac{\hbar^2}{m}\frac{A}{2\pi}\langle r^2\rangle. \tag{31}$$

In the general case $J \neq 0$ one could be interested in the corrections due to the next terms of the expansion of the Bessel functions, that is, in operators that include r_i^{J+2}. This option is possible for every value of J. Or, when the momentum transfer q is not small, the Bessel function $j_J(qr)$ can be taken fully into account with another option (see Section 3.2).

Also in the dipole case, the lowest order term of the isoscalar operator rY_{1M} does not produce a physical excitation, but it simply induces a translation of the whole system. This mode should in principle lie at zero energy and should be decoupled from the physical excitations within RPA, as this theory restores the symmetries broken at the HF level. In practice, as has been discussed extensively in the literature, numerical implementations are not able to realize this symmetry restoration exactly, resulting in the fact that a (usually sizeable) part of the spurious state is contained in one RPA state whose energy is close to, but not identical to, zero. In the present code, the main limitation related to this discussion is the continuum discretization. For a given box in which the system is set, we need a large basis in order to obtain a spurious state close to zero energy: in practical terms, this is illustrated by the numerical results of the left panel of Fig. 1.

For the same reasons, the spurious state is not exactly orthogonal to the other RPA states. To avoid the undesired effect of these overlaps between the spurious state and the physical states, one way is to employ a modified isoscalar dipole operator. This modified operator reads

$$\hat{F}^{(\text{IS dipole})} = \sum_{i=1}^{A}\left(r_i^3 - \eta r_i\right) Y_{1M}(\hat{r}_i), \tag{32}$$

with $\eta = 5\langle r^2\rangle/3$ [25]. The associated double commutator sum rule is

$$m_1 = \frac{\hbar^2}{2m}\frac{A}{4\pi}\left(33\langle r^4\rangle - 25\langle r^2\rangle^2\right). \tag{33}$$

In the right panel of Fig. 1 we show the strength function obtained either with the full operator (32) or without the correction term, that is, with $\eta = 0$. One can see that the spurious strength that needs to be removed is small, and lies mainly in the low-energy region. The spurious state displayed in the left panel is not included in the curves of the right panel.

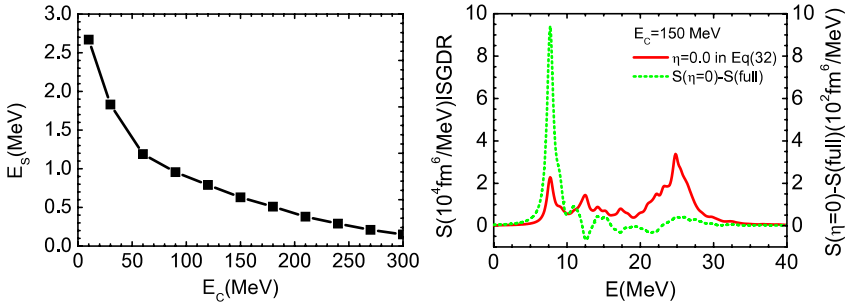

Fig. 1. (Left panel) Energy E_S of the spurious translational state in ^{208}Pb calculated in a box of 24 fm radius with a radial mesh of 0.1 fm. The force is SLy5 [12]. The x-axis shows the cutoff energy E_C. (Right panel) The strength function calculated with the operator without the correction term (that is, with $\eta = 0$) is displayed with the full line. For comparison we also display the difference between this strength function and the exact one by means of the dashed line. It must be noted that the scale for the latter curve (shown on the right side) is two orders of magnitude smaller than the scale for the former curve (shown on the left side). These results correspond to the same physical case and numerical parameters as in the left panel with a cutoff energy of 150 MeV.

In the dipole case, the EWSR associated with the operator (20) should be also provided. It reads

$$m_1 = \frac{9}{4\pi}\frac{\hbar^2}{2m}\frac{NZ}{A}e^2\,(1+\kappa)\,, \tag{34}$$

where κ is the dipole enhancement factor given by

$$\kappa = \frac{2m}{\hbar^2}\frac{A}{4NZ}\left(t_1\left(1+\frac{x_1}{2}\right)+t_2\left(1+\frac{x_2}{2}\right)\right)\int \rho_n(r)\rho_p(r)d^3r. \tag{35}$$

An important remark is now in order. All the Eqs. (26), (29), (31), (33)–(35) in which the nucleon mass m appears have been written in the standard form to allow a straightforward comparison with the available literature. However, we have actually used the corrected mass $m' = m\frac{A}{A-1}$ in the Hartree–Fock calculations as explained after Eq. (6), and therefore the double commutator value of the EWSR must be calculated with m', and m' instead of m should appear in Eqs. (26), (29), (31), (33)–(35).

We end the present section by defining another quantity of interest which characterizes the relationship of each excited state with the ground state. This quantity is the transition density, whose integral with a multipole operator gives the corresponding transition amplitude of that operator. With the help of the $X^{(\nu)}$ and $Y^{(\nu)}$ amplitudes of a given RPA state $|\nu\rangle$, one can construct the radial part of its transition density $\delta\rho_\nu(r)$, which is defined as

$$\begin{aligned}\delta\rho_\nu(\mathbf{r}) &= \langle\nu|\hat{\rho}(\mathbf{r})|\tilde{0}\rangle \\ &= \delta\rho_\nu(r)Y^*_{JM}(\hat{r}).\end{aligned} \tag{36}$$

In terms of the RPA amplitudes the radial transition density of a state $|\nu\rangle$ is

$$\delta\rho_\nu(r) = \frac{1}{\sqrt{2J+1}}\sum_{mi}\left(X^{(\nu)}_{mi}+Y^{(\nu)}_{mi}\right)\langle m||Y_J||i\rangle\frac{u_m(r)u_i(r)}{r^2}, \tag{37}$$

and the summations can be done separately on neutron configurations, or proton configurations, or both. The interest of the transition densities stems from the fact that their spatial shapes reveal the nature of the excitations: volume or surface type, isoscalar or isovector, etc. Moreover, they can be used as input in calculations of inelastic scattering cross sections.

3. How to use the code

We describe here how to enter the parameters in order to run the code. They are contained in the files named `skyrme.in` and `skyrme_rpa.in`, whereas `param.rpa` contains the values of all array dimensions and these values may need to be modified, for instance if the code indicates that some dimension must be increased. If one intends to perform only an HF calculation, the file `skyrme_rpa.in` may contain only the first 5 lines. On the other hand, a complete HF-RPA calculation will require that all 12 lines of `skyrme_rpa.in` contain specified values.

3.1. *The file* `skyrme.in`

This file contains a list of Skyrme parameter sets. Every Skyrme parameterization is included in the form shown in Table 1. The user can add new parameter sets in the file `skyrme.in` by simply making replicas of the existing ones, following the structure displayed in the table. In the present version of the program, the parameters associated with the parameterizations SIII [13], SGII [26], SKM* [27], SkP [28], SkI2 [29], SLy4, SLy5 [12], SkO, SkO′ [30] and LNS [31] can be found.

Two specific comments are in order. One kind of non-standard Skyrme parameterization that can be treated with the present code is the one introduced in Ref. [29], where the spin–orbit term of the energy functional is written as

$$E_{\text{s.o.}} = \int d^3r\left(b_4\mathbf{J}\cdot\boldsymbol{\nabla}\rho + b'_4\sum_q \mathbf{J}_q\cdot\boldsymbol{\nabla}\rho_q\right) \tag{38}$$

instead of the standard form

$$E_{\text{s.o.}} = \int d^3r \, \frac{1}{2} W_0 \left(\mathbf{J} \cdot \boldsymbol{\nabla} \rho + \sum_q \mathbf{J}_q \cdot \boldsymbol{\nabla} \rho_q \right). \tag{39}$$

In the non-standard cases one must give the two quantities $W_0 = 2b_4$ and $W_0' = 2b_4'$, whereas in standard cases one sets W_0' equal to W_0.

The last line in the file `skyrme.in` refers to whether the so-called $\mathbf{J}^2$ terms are included or dropped in HF and RPA. This issue has been briefly discussed in Section 2.1.

3.2. *The file* `skyrme_rpa.in`

The input file must be called `skyrme_rpa.in`. It consists of (maximum) 12 lines, and the input data for each line are described below. It should be noted that both in the input and inside the code the integer numbers, double precision numbers, strings and logical variables are associated with labels starting with `'I'`, `'DP'`, `'S'` and `'B'`, respectively. (The user should be aware that strings, when needed, have a fixed character length.)

Line 1 SSKYRME.
SSKYRME is a string with the acronym of the Skyrme interaction that is used, either pre-existing or to be created. The same string and the associated list of parameters *must* be found in the file `skyrme.in`. Note that there is no default value set by the code.

Line 2 IRADIALMAX, DPSTEP.
IRADIALMAX is the number of points of the radial mesh and DPSTEP is the radial step. If the user sets negative values, these are replaced by default values which are 0.1 fm for the step, and 3 times the nuclear radius $r_0 A^{1/3}$ divided by 0.1 for the number of points (rounded to the nearest integer).

Line 3 DPAA, DPZZ.
These are the values of A and Z of the nucleus. There is no default value.

Line 4 DPDELTAE, INUMITER.
The code iterates the HF procedure until the error on the single-particle energies is smaller than the value DPDELTAE. At most, the number of iterations given by INUMITER is done. If this number is passed and the desired accuracy is not reached, the code continues but displays a warning with the reached accuracy on the single-particle energies. If the user sets a negative value for INUMITER, this is replaced by the default value equal to 500.

Line 5 SPOTENTIAL.
The normal option for this string is `INCLUDE ALL`. If the user wishes to exclude the Coulomb terms, for testing purposes, the available options are: `NO COULOMB`, `NO COULOMB EXCHANGE`. The corresponding terms are dropped both in HF and in RPA. It has to be noted that, prior to the calculations presented in Refs. [8,9], it was usual to retain the Coulomb and spin–orbit terms in HF but exclude them from the residual interaction. This kind of calculation cannot be performed with the present version of the code, but the user could modify the code inside `PHMATRIXELEMENTS`, by retaining the result of the subroutine `SUBPHME` and discarding the outcome of the subroutines `SUBPHME_SO_N`, `SUBPHME_COULOMB` and `SUBPHME_COUL_EXC`.

Line 6 SPURPOSE.
The lines starting from this one (included) up to the end of the input file can be omitted if only HF needs to be performed. If one wishes to perform an RPA calculation the string `SPURPOSE` must be `RPA`. For the parameters in the lines that follow, there are no default values.

Line 7 IISPIN, IPAR.
These parameters correspond to J and to the parity π.

Line 8 IRAD, DPQBESS.
The first parameter is equal to 1 if operators proportional to r_i^J are employed, and 2 in the case of r_i^{J+2}. When $J^\pi = 1^-$ it is possible to set IRAD at 3 and the dipole operators (IS and IV) discussed in Section 2.3 are then employed. If it is set at 4, operators proportional to the Bessel functions $j_J(qr)$ are used. Only in this latter case is the parameter DPQBESS relevant, as it corresponds to q in fm^{-1}.

Line 9 DPEPMAX.
This parameter corresponds to the maximum energy E_C of the unoccupied single-particle states included in the RPA model space (the maximum p–h energy is thus $E_C - \epsilon_h$, where ϵ_h is the deepest hole energy).

Line 10 DPEXINI, DPEXFIN, DPESTEP, DPGAMMA.
The results for the IS and IV strength functions are smeared out with Lorentzian functions with a width DPGAMMA. This averaging is performed between DPEXINI and DPEXFIN and the resulting averaged strengths are listed in steps DPESTEP.

Line 11 SRANGE
Using this line and the next one is optional. If the string `CENTROID ENERGY RANGE` is introduced at line 10, then the code will calculate the centroid energies of the strength function in a range (E_{min}, E_{max}) and these values must be specified in the next line.

Line 12 DPENCENTRMIN, DPENCENTRMAX.
These are E_{min} and E_{max}.

3.3. *The file* `param.rpa`

The parameters associated with the array dimensions are contained in the file `param.rpa` and are listed below.

IP_NNP This must be larger than the number of points in the radial mesh (see line 2 of SKYRMERPA.IN); if not, an error message appears. A standard value is 200, or more.

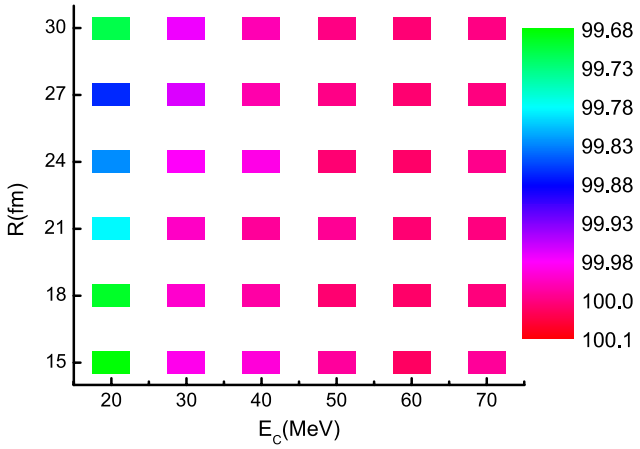

Fig. 2. (Color online) Exhaustion of the energy-weighted sum rule for the IS quadrupole case in ^{208}Pb (using the force SLy5), as a function of the energy cutoff E_C and the size of the box. The different colors correspond to different percentages of the double commutator value, according to the scale given on the right.

IP_ORB In the present version the single-particle states available for either protons or neutrons extend up to $1j_{15/2}$, i.e., 29 orbitals are defined which can accommodate 184 nucleons. The parameter IP_ORB is set accordingly at 29. It has to be noted that this parameter refers only to states occupied at the HF level, so the default value defines the maximum value of N and Z as 184.

IP_NEOC This parameter is set at twice IP_ORB.

IP_IMOREN This is set at 12. It corresponds to the maximum number of unoccupied single-particle levels which can be calculated for each kind of nucleon, and for each (l, j) value. If the value of the cutoff energy is increased, one may need to increase this parameter. In fact, roughly speaking, IP_IMOREN should be larger than E_c plus the Fermi energy, divided by $\hbar\omega = 41A^{-1/3}$. In practice, if the code finds that all the unoccupied states with a given (l, j) value lie below the cutoff energy, it warns that further states below the cutoff may exist and increasing IP_IMOREN should be envisaged.

IP_NSP This must be larger than the total number of single-particle states (occupied plus unoccupied); if not, an error message appears. For orientation, the number of single-particle states below 100 MeV, in ^{208}Pb and with a box radius of 24 fm, is of the order of 450–500 (depending, of course, on the specific Skyrme set).

IP_NCF This must be larger than the number of p–h configurations; if not, an error message appears. For orientation, this value is 2200 if one calculates a large case like $J^\pi = 5^-$ in ^{208}Pb with a box radius of 24 fm and with an energy cutoff of 60 MeV.

3.4. Output files

The main output file is named `skyrme_rpa.out`. Its content should be mostly self-explanatory and an extracted part of the one associated with the test input is provided in Appendix C. Other output files are as follows.

`density.out` This contains the proton and neutron densities (second and third column) at the values of r given in the first column.

`Plot_Bel_*.out` This contains the strength functions averaged with the Lorentzian weights (see above) for the case of the isoscalar (IS), the isovector (IV) and the electromagnetic (EM) operator, respectively.

`td.out` This contains the proton and neutron transition densities (second and third column) for the values of r given in the first column. These are provided for all the RPA states.

The files named `temp*.dat` are temporary files created by each run.

4. Results

We provide in this section some examples of results obtained by using the code. In Appendix B, a typical input file with the associated output file are shown in full detail. We have chosen a case where the output file is short. Accordingly, it should be used as a benchmark for a numerical test after the code has been installed on a computer, but it does not necessarily correspond to the best choice of input parameters from a physical point of view.

4.1. Energy-weighted sum rule exhaustion

In order to give an overall idea of the performance of the code, and present a first set of physical results, we display the exhaustion of the double-commutator EWSR in a two-dimensional plot, as a function of the box radius R and the energy cutoff E_C of the unoccupied states, in Fig. 2. The multipolarity is 2^+, the nucleus is ^{208}Pb, and the Skyrme force is SLy5. From the plot, one can deduce that our implementation of RPA respects the double-commutator sum rule extremely well even for moderate values of the box radius. Of course the results (slightly) improve as the energy cutoff increases. From Fig. 2, one can have an idea of what numerical values of parameters one can use for this example. When one deals with different cases, it should be kept in mind that the optimal box radius values are expected to scale as the nuclear radius ($\sim A^{1/3}$), and the energy cutoff may scale as the shell gap ($\sim A^{-1/3}$).

To see how the EWSR fulfilment evolves with the value of the multipolarity J, we report in Table 2 values for the IS and IV sum rules obtained in the case of ^{208}Pb with the interaction SLy5 (in a spherical box extending up to 24 fm and with E_C equal to 100 MeV), for J ranging from 0 to 5. By increasing J one expects that the strength is moved to higher energies. The same should be true if one looks at IV

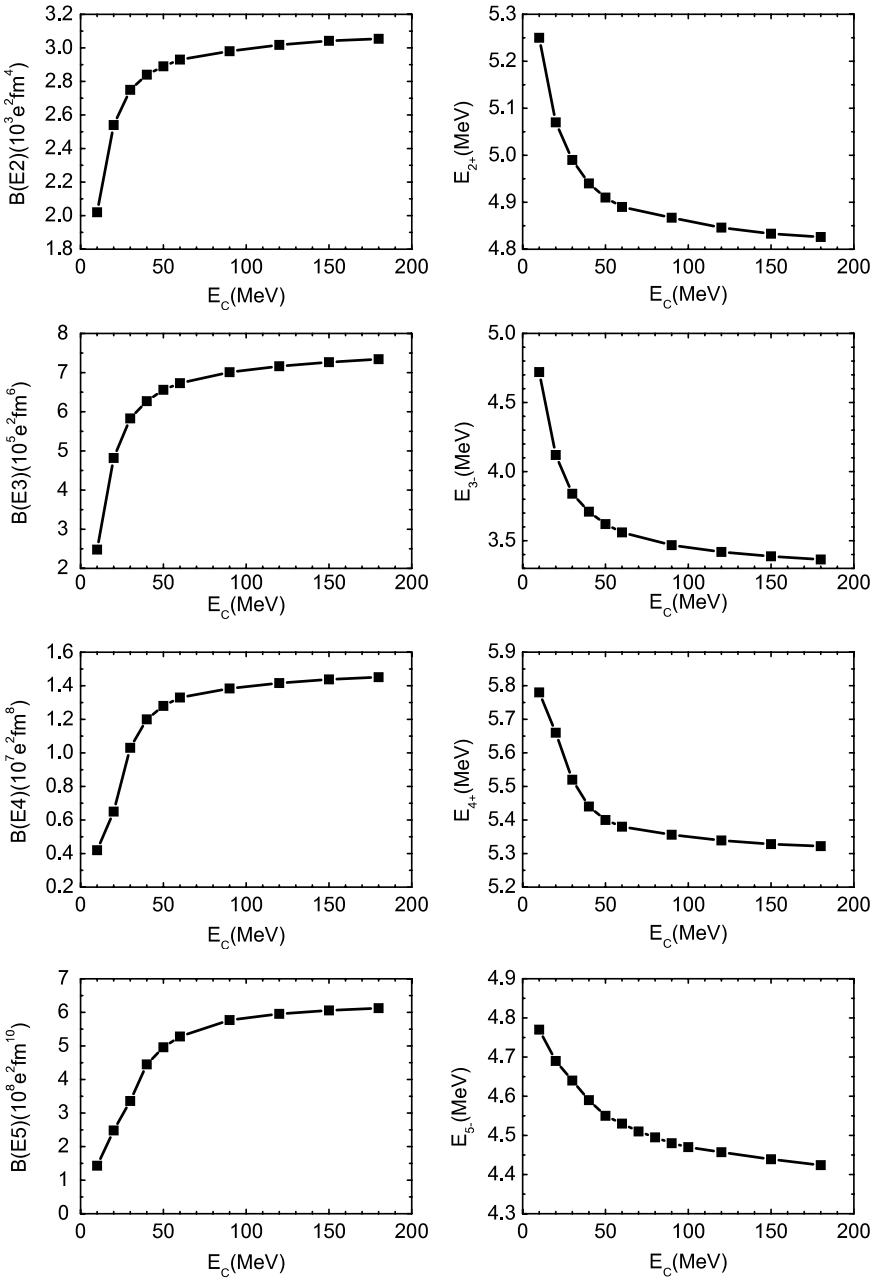

Fig. 3. Low-lying 2^+, 3^-, 4^+, 5^- states in ^{208}Pb calculated in a spherical box extending up to 24 fm and with a radial mesh of 0.1 fm. The parameter set SLy5 [12] is employed. The energies and reduced transition probabilities of the collective low-lying states are shown as a function of the cutoff energy E_C.

instead of IS strength. However, the given model space is large enough so that one can be confident about the sum rule exhaustion. We have also checked that this fact does not depend on the chosen Skyrme interaction. Moreover, we have checked the case of a light nucleus like ^{16}O: also in this case (with the interaction SLy5 and in a spherical box extending up to 14 fm with E_C equal to 200 MeV), the DC value for the EWSR is systematically fulfilled at the level of more than 99.9% for J ranging from 0 to 5.

4.2. Dependence of the results on the model space

In addition to integral properties like the EWSR, assessing the numerical stability of detailed results like the energy and strength of the most collective peaks is among the goals of this section. In fact, one may expect that such properties have a slow convergence as a function of the model space. In fact, the Skyrme interaction is a zero-range force or, strictly speaking, an infinite-range force in the momentum space. Therefore, it is able to provide a coupling between low-energy and rather high-energy p–h configurations. Because of this, the convergence of the properties of vibrational states is expected to be slower with Skyrme forces than with finite-range interactions.

To give a quantitative answer to the question of the convergence as a function of the model space, we display in Fig. 3 the results obtained for both the energy and the electromagnetic transition probabilities of the low-lying states in ^{208}Pb. The convergence is very good in all cases provided the cutoff is large enough (i.e., above 100 MeV).

The same question can be asked for higher-lying states. However, while the low-lying states are below threshold and can be clearly identified independently of the model space, this is not true for states like the giant resonances. These states have a genuine width that

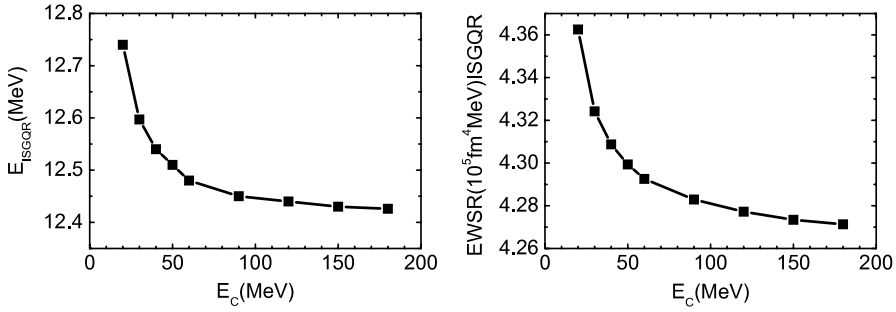

Fig. 4. ISGQR results in ^{208}Pb calculated with a box extending up to 24 fm and a radial mesh of 0.1 fm. The parameter set SLy5 [12] is employed. The centroid energy E_{ISGQR} as well as its total EWSR are shown as a function of the cutoff energy E_C.

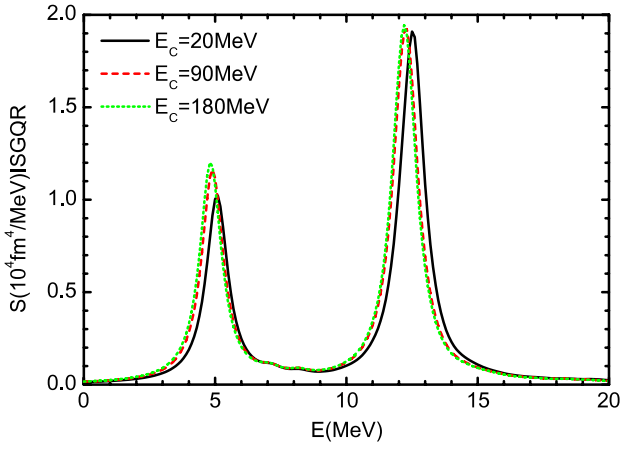

Fig. 5. Isoscalar quadrupole strength in ^{208}Pb calculated with a box extending up to 24 fm and a radial mesh of 0.1 fm. The parameter set SLy5 [12] is employed. The detailed IS quadrupole strength distributions are displayed for different values of the cutoff energy E_C.

includes the Landau and continuum widths (in addition to the spreading width that cannot be accounted for within RPA). Then, if the model space increases, the detailed distribution of eigenstates can vary but we expect that the integral properties converge. By integral properties, we mean the centroid energy and the total fraction of EWSR. These quantities are shown in Fig. 4. Similar considerations as for the low-lying states can be made. The stability of the whole quadrupole strength distributions can also be appreciated by looking at Fig. 5.

4.3. Results for operators carrying finite momentum transfer

As discussed below Eq. (21), the operators introduced in Section 2.3 correspond to the limit of small momentum transfer **q** and they do not depend on the value of **q**. Obviously, in the analysis of any given experiment the proper reaction kinematics is taken into account. Experimentalists usually perform DWBA calculations of inelastic cross sections by using as input a schematic form of the transition densities (36), that only depends on the fraction of isoscalar or isovector strength they exhaust. By matching these calculations and the experimental data, the experimental strength functions are obtained. This method is not free of ambiguities, and calculating directly theoretical inelastic cross sections may be considered preferable.

In spite of these considerations, using operators proportional to the Bessel functions allows having a qualitative hint of how much the strength may be distorted with respect to the case of negligible values of **q**. To take a typical example, α particles with an incident energy of 100–400 MeV scattered at small angles like 2°–5° would correspond to a momentum transfer $q \simeq 0.15$–0.75 fm^{-1}. In Fig. 6 we display results for the IV dipole and IS quadrupole excitations in ^{208}Pb calculated for two finite values of momentum transfer, namely q equal to 0.2 and 0.6 fm^{-1}, respectively.

From Fig. 6 one can see that, by increasing the value of q, the strength is moved to significantly higher energies. In order to describe this high-energy strength, as expected, low values of the energy cutoff E_C are not adequate. However, if E_C is increased enough, one can obtain, for the strength associated with these q-dependent operators, the same kind of accuracy that we have previously discussed.

In Table 3 we display the fulfilment of the EWSR with respect to the double-commutator value, in the case of finite momentum transfer operators. It is evident from the table that the EWSR is satisfied extremely well, as in the case of zero momentum transfer operators.

5. Conclusion

In this work we have presented a code which allows one to compute self-consistently nuclear ground states and excited states in a Hartree–Fock RPA approach, assuming spherical symmetry and using most of the existing parameterizations of the Skyrme interactions. A number of these parameterizations are already built in, and it is easy for the user to add any parameterization not yet included.

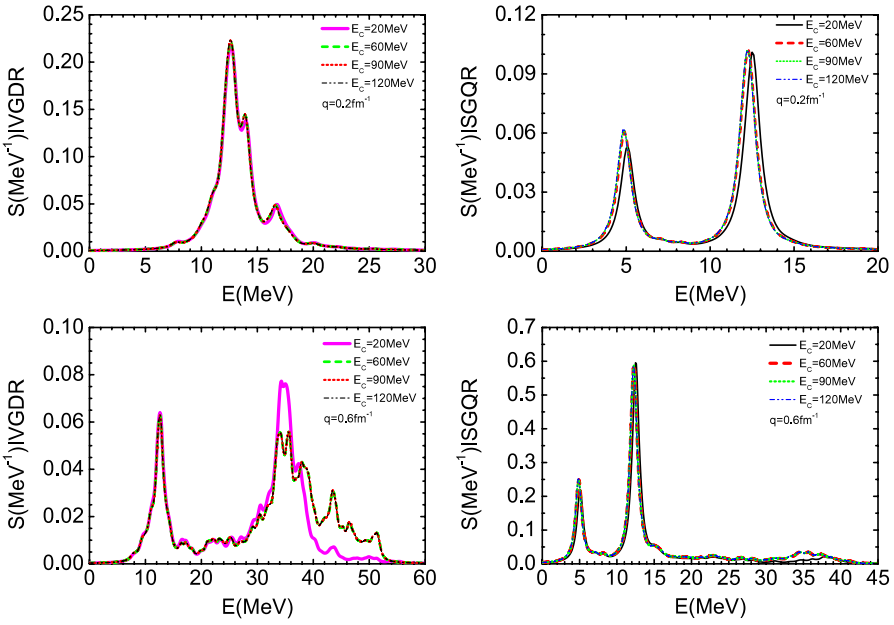

Fig. 6. Strength functions for the IV dipole (left panels) and IS quadrupole (right panels) in ^{208}Pb. The operators are proportional to Bessel functions $j_J(qr)$ and the values of momentum transfer q are displayed. All calculations correspond to the choice of the Skyrme set SLy5 and to a spherical box of 24 fm with a mesh of 0.1 fm.

Table 2
The EWSR m_1 calculated from the RPA states and from the double commutator expectation value, in the case of various multipoles J and for the standard IS ($T = 0$) and IV ($T = 1$) operators (18). The radial functions are $f_J = r^J$ except for $J = 0$ ($f_0 = r^2$), for the isoscalar dipole, $J = 1$ and $T = 0$, where f_J is defined by Eq. (32), and for the isovector dipole, $J = 1$ and $T = 1$, where the operator is given by Eq. (19). The calculations are performed for ^{208}Pb with the Skyrme force SLy5. The box radius and radial mesh are 24 fm and 0.1 fm, respectively. The cutoff energy is 100 MeV. The units are MeV fm^{2J}. R is the ratio m_1 (RPA)/m_1 (D.C.).

J	T	m_1 (RPA)	m_1 (D.C.)	R
0	0	4.20575×10^4	4.20586×10^4	0.99997
	1	4.82499×10^4	4.82537×10^4	0.99992
1	0	5.58732×10^6	5.58727×10^6	1.00001
	1	8.72686×10^3	8.72710×10^3	0.99997
2	0	5.25741×10^5	5.25733×10^5	1.00002
	1	6.03113×10^5	6.03172×10^5	0.99990
3	0	6.09373×10^7	6.09348×10^7	1.00004
	1	6.80859×10^7	6.80949×10^7	0.99987
4	0	6.21181×10^9	6.21154×10^9	1.00004
	1	6.77487×10^9	6.77632×10^9	0.99979
5	0	6.12605×10^{11}	6.12634×10^{11}	0.99995
	1	6.53799×10^{11}	6.53977×10^{11}	0.99972

Besides the spherical symmetry assumption, additional physics limitations imposed to the code are enumerated in the introduction and the users should be aware of them. Apart from that, the code is made as automatic as it can be so that one does not need to be a Hartree–Fock or an RPA practitioner to perform the calculations and to understand the results.

In the write-up we have explained the main steps of the calculations, at both the Hartree–Fock and RPA levels. Some details about the expressions of the particle–hole matrix elements are given in Appendix A. Throughout the whole numerical process the full self-consistency between the mean field calculations and RPA calculations is maintained, which means that even in the options "no Coulomb" or "no Coulomb exchange", the full Coulomb contributions or the Coulomb exchange contributions are simultaneously turned off in Hartree–Fock and RPA. This self-consistency is controlled in the outputs by comparing the linear EWSR with the double commutator expectation value.

With this `skyrme_rpa` code we hope that the RPA models based on Skyrme-type interactions will become accessible to an even wider part of the nuclear physics community.

Acknowledgments

We would like to thank H.Z. Liang for his help in the derivation of the $\mathbf{J}^2$ part of the residual interaction, and M. Brenna, D. Gambacurta and G. Pozzi for their careful reading of the manuscript. G.C. acknowledges the hospitality and support of Institute of Modern Physics, Lanzhou, where part of this work was done. C.L. acknowledges the support of the UniAMO fellowship provided by Fondazione Cariplo and

Table 3
The same as Table 2 in the case of finite momentum transfer $q = 0.2$ fm^{-1}, for various multipoles J and for the standard IS ($T = 0$) and IV ($T = 1$) operators. The units are MeV and R is the ratio m_1 (RPA)/m_1 (D.C.).

J	T	m_1 (RPA)	m_1 (D.C.)	R
0	0	1.36405	1.36418	0.99991
	1	1.57787	1.56415	1.00877
1	0	9.27290	9.27290	1.00000
	1	11.0583	10.9374	1.01105
2	0	2.73901	2.73892	1.00003
	1	3.16752	3.14042	1.00863
3	0	0.272107	0.272089	1.00007
	1	0.305934	0.303907	1.00667
4	0	1.41045×10^{-2}	1.41035×10^{-2}	1.00007
	1	1.54603×10^{-2}	1.53797×10^{-2}	1.00524
5	0	4.67273×10^{-4}	4.67332×10^{-4}	0.99987
	1	5.00760×10^{-4}	4.98718×10^{-4}	1.00409

Università degli Studi which allowed his stay in Milano, and the support of the National Natural Science Foundation of China under Grant Nos. 10875150 and 11175216.

Appendix A. The particle–hole residual interaction and its matrix elements

We discuss separately in the following subsections the p–h matrix elements of (i) the terms of the residual interaction proportional to the Skyrme parameters t_0 and t_3 (i.e., momentum-independent), (ii) the terms proportional to t_1 and t_2 (i.e., momentum-dependent), (iii) the spin–orbit term, (iv) the Coulomb and Coulomb-exchange terms. The p–h matrix elements are defined by Eq. (16). For the sake of simplicity, we use here the notation $H_J(abcd)$ instead of $\langle \overbrace{a\underbrace{b|V_{res}|c}_{J}d}^{J}\rangle$. Moreover, in this appendix, the label qq (qq') denotes the interaction between p–h pairs of the same (different) charge.

A.1. Momentum-independent terms

As discussed in Section 2.2, the antisymmetrized p–h interaction proportional to t_0 and t_3 must be derived from Eq. (17). The result is

$$V_{res}^{qq} = v_0^{qq}\delta(\mathbf{r}_1-\mathbf{r}_2) + v_\sigma^{qq}\delta(\mathbf{r}_1-\mathbf{r}_2)\boldsymbol{\sigma}_1\cdot\boldsymbol{\sigma}_2,$$
$$V_{res}^{qq'} = v_0^{qq'}\delta(\mathbf{r}_1-\mathbf{r}_2) + v_\sigma^{qq'}\delta(\mathbf{r}_1-\mathbf{r}_2)\boldsymbol{\sigma}_1\cdot\boldsymbol{\sigma}_2. \tag{A.1}$$

The functions v depend only on the radial coordinate r, and their detailed expressions are

$$\begin{aligned}
v_0^{qq}(r) &= \frac{1}{2}t_0(1-x_0) + \frac{1}{16}t_3(\alpha+2)(\alpha+1)\rho^\alpha(r) - \frac{1}{12}t_3\left(x_3+\frac{1}{2}\right)\rho^\alpha(r) + \frac{1}{48}t_3\alpha(1-\alpha)(1+2x_3)\rho^{\alpha-2}(r)\rho_-^2(r)\\
&\quad - \frac{1}{12}t_3(2x_3+1)\alpha\rho^{\alpha-1}(r)\rho_-(r),\\
v_0^{qq'}(r) &= \frac{1}{2}t_0(2+x_0) + \frac{1}{16}t_3(\alpha+2)(\alpha+1)\rho^\alpha(r) + \frac{1}{12}t_3\left(x_3+\frac{1}{2}\right)\rho^\alpha(r) + \frac{1}{48}t_3\alpha(1-\alpha)(1+2x_3)\rho^{\alpha-2}(r)\rho_-^2(r),\\
v_\sigma^{qq}(r) &= \frac{1}{2}t_0(x_0-1) - \frac{1}{12}t_3(1-x_3)\rho^\alpha(r),\\
v_\sigma^{qq'}(r) &= \frac{1}{2}t_0x_0 + \frac{1}{12}t_3x_3\rho^\alpha(r).
\end{aligned} \tag{A.2}$$

In these formulas ρ_- stands for $\rho_n - \rho_p$.

Both for the qq and qq' cases the direct p–h matrix element reads

$$\begin{aligned}
H_J(abcd) &= \frac{1}{2J+1}\langle a||Y_J||c\rangle\langle d||Y_J||b\rangle\int\frac{dr}{r^2}v_0(r)u_a(r)u_b(r)u_c(r)u_d(r) + \frac{1}{2J+1}\sum_L\langle a|\left|[Y_L\otimes\boldsymbol{\sigma}]_J\right||c\rangle\langle d|\left|[Y_L\otimes\boldsymbol{\sigma}]_J\right||b\rangle\\
&\quad\times\int\frac{dr}{r^2}v_\sigma(r)u_a(r)u_b(r)u_c(r)u_d(r).
\end{aligned} \tag{A.3}$$

A.2. Momentum-dependent terms

The antisymmetrized p–h interaction corresponding to the t_1, t_2 terms can be written as

$$\widetilde{V}(\mathbf{r}_1,\mathbf{r}_2) = \frac{t_1}{2}(\mathbf{P}'^2\delta+\delta\mathbf{P}^2)(1+x_1P_\sigma)(1-P_\sigma P_\tau) + t_2\mathbf{P}'\cdot\delta\mathbf{P}(1+x_2P_\sigma)(1+P_\sigma P_\tau), \tag{A.4}$$

with the notation of Section 2.1.

Table A.1
The operators and numerical coefficients of Eq. (A.5).

i	$v^{(i)}$	$\alpha_i^{(qq)}$	$\beta_i^{(qq)}$	$\alpha_i^{(qq')}$	$\beta_i^{(qq')}$
1	$(\overleftarrow{\nabla}_1^2+\overleftarrow{\nabla}_2^2)\delta+\delta(\overrightarrow{\nabla}_1^2+\overrightarrow{\nabla}_2^2)$	$\left(\frac{x_1}{2}-\frac{1}{2}\right)\frac{t_1}{8}$	$\left(\frac{1}{2}-\frac{x_1}{2}\right)\frac{t_1}{8}$	$\left(-1-\frac{x_1}{2}\right)\frac{t_1}{8}$	$-\frac{x_1}{2}\frac{t_1}{8}$
2	$\overleftarrow{\nabla}_1\cdot\overleftarrow{\nabla}_2\delta$	$\left(\frac{1}{2}-\frac{x_1}{2}\right)\frac{t_1}{4}$	$\left(\frac{x_1}{2}-\frac{1}{2}\right)\frac{t_1}{4}$	$\left(1+\frac{x_1}{2}\right)\frac{t_1}{4}$	$\frac{x_1}{2}\frac{t_1}{4}$
3	$\delta\overrightarrow{\nabla}_1\cdot\overrightarrow{\nabla}_2$	$\alpha_2^{(qq)}$	$\beta_2^{(qq)}$	$\alpha_2^{(qq')}$	$\beta_2^{(qq')}$
4	$\overleftarrow{\nabla}_1\cdot\delta\overrightarrow{\nabla}_2$	$-\left(\frac{3}{2}+\frac{3x_2}{2}\right)\frac{t_2}{4}$	$-\left(\frac{x_2}{2}+\frac{1}{2}\right)\frac{t_2}{4}$	$-\left(1+\frac{x_2}{2}\right)\frac{t_2}{4}$	$-\frac{x_2}{2}\frac{t_2}{4}$
5	$\overleftarrow{\nabla}_2\cdot\delta\overrightarrow{\nabla}_1$	$\alpha_4^{(qq)}$	$\beta_4^{(qq)}$	$\alpha_4^{(qq')}$	$\beta_4^{(qq')}$
6	$\overleftarrow{\nabla}_1\cdot\delta\overrightarrow{\nabla}_1$	$-\alpha_4^{(qq)}$	$-\beta_4^{(qq)}$	$-\alpha_4^{(qq')}$	$-\beta_4^{(qq')}$
7	$\overleftarrow{\nabla}_2\cdot\delta\overrightarrow{\nabla}_2$	$-\alpha_4^{(qq)}$	$-\beta_4^{(qq)}$	$-\alpha_4^{(qq')}$	$-\beta_4^{(qq')}$

Denoting by (l_a, j_a) the quantum numbers of a single-particle state, the p–h matrix elements of the interaction (A.4) have the general form (both for qq and qq' pairs)

$$H_J(abcd)=\sum_i \alpha_i H_J^{0(i)}(abcd)+\sum_i \beta_i H_J^{\sigma(i)}(abcd). \tag{A.5}$$

The coefficients α_i and β_i are combinations of the Skyrme parameters. They correspond to the seven operators of Table A.1. The functions $H_J^{0(i)}(abcd)$ and $H_J^{\sigma(i)}(abcd)$ are defined as

$$\begin{aligned}
H_J^{0(i)}(abcd) &= (-1)^{l_a+j_b+l_d+j_c+1}\widehat{j_a j_b j_c j_d}\begin{Bmatrix} j_a & l_a & \frac{1}{2}\\ l_c & j_c & J\end{Bmatrix}\begin{Bmatrix} j_d & l_d & \frac{1}{2}\\ l_b & j_b & J\end{Bmatrix} v_J^{(i)}(abcd),\\
H_J^{\sigma(i)}(abcd) &= 6\widehat{j_a j_b j_c j_d}\sum_L \widehat{L}^2\begin{Bmatrix} j_a & l_a & \frac{1}{2}\\ j_c & l_c & \frac{1}{2}\\ J & L & 1\end{Bmatrix}\begin{Bmatrix} j_d & l_d & \frac{1}{2}\\ j_b & l_b & \frac{1}{2}\\ J & L & 1\end{Bmatrix} v_L^{(i)}(abcd).
\end{aligned} \tag{A.6}$$

We finally need the seven functions $v_L^{(i)}(abcd)$ which can be calculated with the following expressions. The first function $v_L^{(1)}(abcd)$ reads

$$v_L^{(1)}(abcd)=\widehat{L}^{-2} I_1(abcd)\langle l_a\|Y_L\|l_c\rangle\langle l_d\|Y_L\|l_b\rangle, \tag{A.7}$$

with

$$\langle l_a\|Y_L\|l_c\rangle=(-1)^{\widetilde{l_a}}\frac{\widehat{l_a l_c L}}{\sqrt{4\pi}}\begin{pmatrix} l_a & l_c & L\\ 0 & 0 & 0\end{pmatrix} \tag{A.8}$$

and

$$I_1(abcd)=\int \frac{dr}{r^2}\left[\left(u_a''-\frac{l_a(l_a+1)}{r^2}u_a\right)u_b u_c u_d+3\text{ other terms}\right]. \tag{A.9}$$

The second function $v_L^{(2)}(abcd)$ is

$$\begin{aligned}
v_L^{(2)}(abcd) &= \sum_{KK'\Lambda}(-1)^{L+K+K'}\widehat{l_a l_b K K'}\begin{pmatrix} K & l_a & 1\\ 0 & 0 & 0\end{pmatrix}\begin{pmatrix} K' & l_b & 1\\ 0 & 0 & 0\end{pmatrix}\begin{Bmatrix} \Lambda & 1 & L\\ l_a & l_c & K\end{Bmatrix}\begin{Bmatrix} \Lambda & 1 & L\\ l_b & l_d & K'\end{Bmatrix}\\
&\quad\times I_2(KK';abcd)\langle l_c\|Y_\Lambda\|K\rangle\langle l_d\|Y_\Lambda\|K'\rangle,
\end{aligned} \tag{A.10}$$

where

$$I_2(KK';abcd)=\int dr\left[D_K\left(\frac{u_a}{r}\right)\right]\left[D_{K'}\left(\frac{u_b}{r}\right)\right]u_c u_d \tag{A.11}$$

and

$$D_K\left(\frac{u_a}{r}\right)=\begin{cases}\left(\dfrac{d}{dr}-\dfrac{l_a}{r}\right)\dfrac{u_a}{r} & \text{if } K=l_a+1\\ \left(\dfrac{d}{dr}+\dfrac{l_a+1}{r}\right)\dfrac{u_a}{r} & \text{if } K=l_a-1.\end{cases} \tag{A.12}$$

The functions $v_L^{(3)}$, $v_L^{(4)}$, $v_L^{(5)}$ are given by

$$\begin{aligned}
v_L^{(3)}(abcd) &= v_L^{(2)}(dcba)\\
v_L^{(4)}(abcd) &= (-1)^L v_L^{(2)}(acbd)\\
v_L^{(5)}(abcd) &= (-1)^L v_L^{(2)}(bdac).
\end{aligned} \tag{A.13}$$

Table A.2
The numerical coefficients of Eq. (A.5) associated to the $\mathbf{J}^2$ part of the residual interaction.

i	$v^{(i)}$	$\beta_i^{(qq)}$	$\beta_i^{(qq')}$
1	$\overleftarrow{\nabla}_1\overleftarrow{\nabla}_2\delta(\overrightarrow{r})$	$\frac{1}{16}(-t_1+t_2-t_1x_1+t_2x_2)$	$\frac{1}{16}(-t_1x_1+t_2x_2)$
2	$\delta(\overrightarrow{r})\overrightarrow{\nabla}_1\overrightarrow{\nabla}_2$	$\beta_1^{(qq)}$	$\beta_1^{(qq')}$
3	$\overleftarrow{\nabla}_1\delta(\overrightarrow{r})\overrightarrow{\nabla}_2$	$-\beta_1^{(qq)}$	$-\beta_1^{(qq')}$
4	$\overleftarrow{\nabla}_2\delta(\overrightarrow{r})\overrightarrow{\nabla}_1$	$-\beta_1^{(qq)}$	$-\beta_1^{(qq')}$
5	$\overleftarrow{\nabla}_1\delta(\overrightarrow{r})\overrightarrow{\nabla}_1$	$2\beta_1^{(qq)}$	$2\beta_1^{(qq')}$
6	$\overleftarrow{\nabla}_2\delta(\overrightarrow{r})\overrightarrow{\nabla}_2$	$2\beta_1^{(qq)}$	$2\beta_1^{(qq')}$

Finally, the functions $v_L^{(6)}$ and $v_L^{(7)}$ can be obtained by

$$v_L^{(6)}(abcd) = \sum_{KK'} \widehat{L}^{-2}\widehat{l_a}\widehat{l_c}\widehat{K}\widehat{K'} \begin{pmatrix} K & l_a & 1 \\ 0 & 0 & 0 \end{pmatrix} \begin{pmatrix} K' & l_c & 1 \\ 0 & 0 & 0 \end{pmatrix} \begin{Bmatrix} K' & K & L \\ l_a & l_c & 1 \end{Bmatrix} I_2(KK';adbc)\langle K\|Y_L\|K'\rangle\langle l_b\|Y_L\|l_d\rangle,$$
$$v_L^{(7)}(abcd) = v_L^{(6)}(badc). \tag{A.14}$$

As mentioned in the main text, when the $\mathbf{J}^2$ terms are dropped this is done both at the mean-field level and in the p–h residual interaction. They are dropped together with the so-called $\mathbf{s}\cdot\mathbf{T}$ terms since only the combination $\mathbf{s}\cdot\mathbf{T}-\mathbf{J}^2$ preserves the gauge invariance (see Ref. [32] for a discussion on this point, and the definition of all generalized densities including $\mathbf{s}(\mathbf{r})$ and $\mathbf{T}(\mathbf{r})$). This amounts to a change of the coefficients of Eq. (A.5). For convenience, we list the coefficients associated to the part of the residual interaction that is dropped in Table A.2.

A.3. Spin–orbit term

The spin–orbit term has a more complicated structure. We give here the necessary expressions for calculating the direct p–h matrix elements. The exchange matrix elements can be expressed as linear combinations of appropriate direct matrix elements, as usual. We write

$$\begin{aligned} V_{\text{s.o.}} &= \frac{i}{4}W_0\left[(\boldsymbol{\sigma}_1-\boldsymbol{\sigma}_2)(\overleftarrow{\nabla}_1-\overleftarrow{\nabla}_2)\delta(\mathbf{r}_1-\mathbf{r}_2)\times(\overrightarrow{\nabla}_1-\overrightarrow{\nabla}_2)\right] \\ &= \frac{i}{4}W_0\sum_{i=1}^{8}w^{(i)}, \end{aligned} \tag{A.15}$$

and the eight terms in the sum are

$$\begin{aligned} w^{(1)} &= \overrightarrow{\boldsymbol{\sigma}}_1\cdot\overleftarrow{\nabla}_1\delta(\mathbf{r}_1-\mathbf{r}_2)\times\overrightarrow{\nabla}_1 & w^{(5)} &= -\overrightarrow{\boldsymbol{\sigma}}_1\cdot\overleftarrow{\nabla}_1\delta(\mathbf{r}_1-\mathbf{r}_2)\times\overrightarrow{\nabla}_2 \\ w^{(2)} &= -\boldsymbol{\sigma}_1\cdot\overleftarrow{\nabla}_2\delta(\mathbf{r}_1-\mathbf{r}_2)\times\overrightarrow{\nabla}_1 & w^{(6)} &= \boldsymbol{\sigma}_1\cdot\overleftarrow{\nabla}_2\delta(\mathbf{r}_1-\mathbf{r}_2)\times\overrightarrow{\nabla}_2 \\ w^{(3)} &= \boldsymbol{\sigma}_2\cdot\overleftarrow{\nabla}_1\delta(\mathbf{r}_1-\mathbf{r}_2)\times\overrightarrow{\nabla}_1 & w^{(7)} &= -\boldsymbol{\sigma}_2\cdot\overleftarrow{\nabla}_1\delta(\mathbf{r}_1-\mathbf{r}_2)\times\overrightarrow{\nabla}_2 \\ w^{(4)} &= -\boldsymbol{\sigma}_2\cdot\overleftarrow{\nabla}_2\delta(\mathbf{r}_1-\mathbf{r}_2)\times\overrightarrow{\nabla}_1 & w^{(8)} &= \boldsymbol{\sigma}_2\cdot\overleftarrow{\nabla}_2\delta(\mathbf{r}_1-\mathbf{r}_2)\times\overrightarrow{\nabla}_2. \end{aligned} \tag{A.16}$$

The coupled p–h matrix elements of the eight operators $w^{(i)}$ are labelled by $H_J^{w(i)}(abcd)$ and are given by the following expressions:

$$\begin{aligned} H_J^{w(1)}(abcd) &= (-1)^{-\frac{1}{2}-l_b+j_b}\frac{\sqrt{2}\sqrt{6}\sqrt{3}}{4(2J+1)}\widehat{j_a}\widehat{j_b}\widehat{j_c}\widehat{j_d}\begin{Bmatrix} j_d & j_b & J \\ l_b & l_d & \frac{1}{2}\end{Bmatrix}\sum_{k,i}(-1)^{\frac{k}{2}+\frac{i}{2}-k}\left(l_a+\frac{k}{2}+\frac{1}{2}\right)^{\frac{1}{2}}\left(l_c+\frac{i}{2}+\frac{1}{2}\right)^{\frac{1}{2}} \\ &\times\langle l_a+k\|Y_J\|l_c+i\rangle\langle l_b\|Y_J\|l_d\rangle\int dr r^2\phi_b(r)\phi_d(r)D_k\phi_a(r)D_i\phi_c(r) \\ &\times\sum_{\Lambda}(-1)^{\Lambda}(2\Lambda+1)\begin{Bmatrix} J & \Lambda & 1 \\ l_c+i & l_c & 1 \\ l_a+k & l_a & 1\end{Bmatrix}\begin{Bmatrix} l_a & \Lambda & l_c \\ j_a & J & j_c \\ \frac{1}{2} & 1 & \frac{1}{2}\end{Bmatrix} \end{aligned} \tag{A.17}$$

$$\begin{aligned} H_J^{w(2)}(abcd) &= (-1)^{\frac{1}{2}-j_b+J-l_d}\frac{\sqrt{2}\sqrt{3}\sqrt{6}}{4}\widehat{j_a}\widehat{j_b}\widehat{j_c}\widehat{j_d}\begin{Bmatrix} l_b & l_d & J \\ j_d & j_b & \frac{1}{2}\end{Bmatrix}\sum_{k,i}(-1)^{\frac{i}{2}+\frac{k}{2}-k}\left(l_b+\frac{k}{2}+\frac{1}{2}\right)^{\frac{1}{2}}\left(l_c+\frac{i}{2}+\frac{1}{2}\right)^{\frac{1}{2}} \\ &\times\int dr r^2\phi_a(r)D_i\phi_c(r)\phi_d(r)D_k\phi_b(r)\sum_{\alpha}\langle l_a\|Y_\alpha\|l_c+i\rangle\langle l_b+k\|Y_\alpha\|l_d\rangle \\ &\times\begin{Bmatrix}\alpha & 1 & J \\ l_b & l_d & l_b+k\end{Bmatrix}\sum_{\Lambda}(-1)^{-\Lambda}\widehat{\Lambda}^2\begin{Bmatrix} J & \alpha & 1 \\ 1 & 1 & \Lambda\end{Bmatrix}\begin{Bmatrix} l_a & \Lambda & l_c \\ j_a & J & j_c \\ \frac{1}{2} & 1 & \frac{1}{2}\end{Bmatrix}\begin{Bmatrix} 1 & \alpha & \Lambda \\ l_a & l_c & l_c+i\end{Bmatrix} \end{aligned} \tag{A.18}$$

$$H_J^{w(3)}(abcd) = (-1)^{\frac{1}{2}+J-j_c-l_c}\frac{\sqrt{2}\sqrt{3}\sqrt{6}}{4}\widehat{j_a}\widehat{j_b}\widehat{j_c}\widehat{j_d}\begin{Bmatrix} l_a & l_c & J \\ j_c & j_a & \frac{1}{2}\end{Bmatrix}\sum_{k,i}(-1)^{\frac{k}{2}+\frac{i}{2}-i}\left(l_a+\frac{k}{2}+\frac{1}{2}\right)^{\frac{1}{2}}\left(l_c+\frac{i}{2}+\frac{1}{2}\right)^{\frac{1}{2}}$$
$$\times\int dr r^2\phi_b(r)\phi_d(r)D_k\phi_a(r)D_i\phi_c(r)\sum_\alpha\langle l_a+k\|Y_\alpha\|l_c+i\rangle\langle l_b\|Y_\alpha\|l_d\rangle\begin{Bmatrix} l_d & \alpha & l_b \\ j_d & J & j_b \\ \frac{1}{2} & 1 & \frac{1}{2}\end{Bmatrix}\begin{Bmatrix} \alpha & J & 1 \\ l_c+i & l_c & 1 \\ l_a+k & l_a & 1\end{Bmatrix} \quad (A.19)$$

$$H_J^{w(4)}(abcd) = (-1)^{\frac{1}{2}-j_c+l_c+j_d+j_b}\frac{\sqrt{2}\sqrt{3}\sqrt{6}}{4}\widehat{j_a}\widehat{j_b}\widehat{j_c}\widehat{j_d}\begin{Bmatrix} l_a & l_c & J \\ j_c & j_a & \frac{1}{2}\end{Bmatrix}\sum_{i,k}(-1)^{\frac{i}{2}+\frac{k}{2}+i}\left(l_c+\frac{i}{2}+\frac{1}{2}\right)^{\frac{1}{2}}\left(l_b+\frac{k}{2}+\frac{1}{2}\right)^{\frac{1}{2}}$$
$$\times\int dr r^2\phi_a(r)D_i\phi_c(r)\phi_d(r)D_k\phi_b(r)\sum_\alpha\begin{Bmatrix} 1 & \alpha & J \\ l_a & l_c & l_c+i\end{Bmatrix}\langle l_a\|Y_\alpha\|l_c+i\rangle\langle l_b+k\|Y_\alpha\|l_d\rangle$$
$$\times\sum_\Lambda\widehat{\Lambda}^2\begin{Bmatrix} l_b & \Lambda & l_d \\ j_b & J & j_d \\ \frac{1}{2} & 1 & \frac{1}{2}\end{Bmatrix}\begin{Bmatrix}\Lambda & \alpha & 1 \\ 1 & 1 & J\end{Bmatrix}\begin{Bmatrix} 1 & \alpha & \Lambda \\ l_d & l_b & l_b+k\end{Bmatrix} \quad (A.20)$$

$$H_J^{w(5)}(abcd) = (-1)^{1-j_a-j_b+j_c-j_d}\times H_J^{w(4)}(badc) \quad (A.21)$$

$$H_J^{w(6)}(abcd) = (-1)^{1+j_a-j_b+j_c+j_d}\times H_J^{w(3)}(badc) \quad (A.22)$$

$$H_J^{w(7)}(abcd) = (-1)^{1+j_a+j_b+j_c-j_d}\times H_J^{w(2)}(badc) \quad (A.23)$$

$$H_J^{w(8)}(abcd) = (-1)^{1-j_a+j_b+j_c+j_d}\times H_J^{w(1)}(badc). \quad (A.24)$$

A.4. Coulomb terms

The direct matrix element of the Coulomb interaction between protons reads

$$H_J(abcd) = \frac{4\pi e^2}{(2J+1)^2}\langle a||Y_J||c\rangle\langle d||Y_J||b\rangle\int dr_1 dr_2\frac{r_<^J}{r_>^{J+1}}u_a(r_1)u_b(r_2)u_c(r_1)u_d(r_2), \quad (A.25)$$

where $r_>$ ($r_<$) stands for the larger (smaller) among r_1, r_2.

The exchange matrix element must be consistent with the Slater approximation in the mean field; therefore it is derived from Eq. (17) starting from Eq. (4). The result is

$$V_{CX} = -\frac{1}{3}e^2\left(\frac{3}{\pi}\right)^{\frac{1}{3}}\rho_p(r)^{-\frac{2}{3}}\delta(\mathbf{r}_1-\mathbf{r}_2) = v_{CX}(r)\delta(\mathbf{r}_1-\mathbf{r}_2), \quad (A.26)$$

and the p–h matrix element is

$$H_J(abcd) = \frac{1}{2J+1}\langle a||Y_J||c\rangle\langle d||Y_J||b\rangle\int\frac{dr}{r^2}v_{CX}(r)u_a(r)u_b(r)u_c(r)u_d(r). \quad (A.27)$$

Appendix B. Test run input

```
SLy5
150 0.10
16 8
0.0001 300
INCLUDE ALL
RPA
3 -1
1 0.0
50
0. 60.0 0.1 1.0
CENTROID ENERGY RANGE
0. 60.
```

Appendix C. Test run output

For convenience, only a selected part of the complete output is reported. In it, all lengths are in fm and all energies in MeV.

```
HARTREE-FOCK FOR THE NUCLEUS A= 16 AND Z= 8
SKYRME PARAMETER SET: SLy5
RPA FOR J AND PARITY: 3 -1
**********************************************************************
```

```
********************************************************************************
FULL HF POTENTIAL INCLUDED
NUMBER OF POINTS AND MESH: 150 0.1000
********************************************************************************
CONVERGENCE REACHED AFTER 53 ITERATIONS
AT THE DESIRED ACCURACY 0.95317E-04
********************************************************************************
PROTON STATES
i n l j Energy
1 1 0 1/2 -0.32346E+02
2 1 1 3/2 -0.17138E+02
3 1 1 1/2 -0.11083E+02
NEUTRON STATES
i n l j Energy
4 1 0 1/2 -0.36138E+02
5 1 1 3/2 -0.20613E+02
6 1 1 1/2 -0.14429E+02
********************************************************************************
[...]
ETot/A=-0.80261107E+01

RN= 0.26585E+01
RP= 0.26836E+01
RC= 0.27991E+01


GROUND STATES EXPECTATION VALUES
L <r^(2L-2)>
1 0.10000E+01
2 0.71346E+01
3 0.77075E+02
4 0.11566E+04
5 0.23860E+05
6 0.68710E+06
7 0.27920E+08

[...]
OPERATORS PROPORTIONAL TO r**J ARE EMPLOYED


****************************** RPA STATES ******************************

    E           B(IS)       %M0(IS)     B(EM)       B(IV)       %M0(IV)
--------------------------------------------------------------------------

 1 0.68161E+01 0.24902E+04 0.20785E+02 0.67271E+03 0.38882E+01 0.44560E-01
 2 0.96349E+01 0.87962E+00 0.73420E-02 0.15234E+03 0.65655E+03 0.75242E+01
 3 0.14017E+02 0.14612E+04 0.12196E+02 0.45519E+03 0.19758E+02 0.22643E+00
 4 0.15142E+02 0.60363E+01 0.50384E-01 0.11384E+03 0.56625E+03 0.64894E+01
 5 0.15314E+02 0.68728E+02 0.57366E+00 0.78807E+01 0.71595E+01 0.82050E-01
 6 0.17428E+02 0.38479E+02 0.32117E+00 0.81278E-04 0.38703E+02 0.44354E+00
 7 0.17954E+02 0.13497E+03 0.11265E+01 0.10447E+03 0.77867E+02 0.89237E+00
 8 0.18355E+02 0.17899E+04 0.14940E+02 0.51526E+03 0.95584E+01 0.10954E+00
 9 0.20203E+02 0.49695E+02 0.41480E+00 0.36249E-01 0.55209E+02 0.63271E+00
10 0.20390E+02 0.11016E+03 0.91948E+00 0.88223E+02 0.68719E+02 0.78754E+00
11 0.21120E+02 0.25631E+02 0.21394E+00 0.36947E+02 0.29652E+03 0.33981E+01
12 0.21348E+02 0.85195E+01 0.71110E-01 0.74759E+01 0.65005E+01 0.74498E-01
13 0.22253E+02 0.50053E+02 0.41779E+00 0.24960E+02 0.85098E+01 0.97524E-01
14 0.22393E+02 0.27120E+02 0.22636E+00 0.79883E+02 0.53283E+03 0.61064E+01
15 0.23618E+02 0.69018E+01 0.57608E-01 0.55127E-01 0.95896E+01 0.10990E+00
16 0.23938E+02 0.63726E+02 0.53191E+00 0.14760E+02 0.89538E-01 0.10261E-02
17 0.24008E+02 0.30407E+02 0.25380E+00 0.33520E+02 0.36785E+02 0.42157E+00
18 0.24012E+02 0.13713E+01 0.11446E-01 0.25013E+01 0.39683E+01 0.45478E-01
19 0.24122E+02 0.25740E+03 0.21485E+01 0.29891E+03 0.34351E+03 0.39368E+01
20 0.26091E+02 0.29142E+03 0.24325E+01 0.11431E+00 0.26879E+03 0.30805E+01
21 0.26381E+02 0.33760E+02 0.28179E+00 0.44964E-01 0.29012E+02 0.33248E+00
```

```
22 0.26387E+02 0.12907E+01 0.10773E-01 0.84978E-03 0.14265E+01 0.16348E-01
23 0.26490E+02 0.20569E+02 0.17169E+00 0.24128E+02 0.27972E+02 0.32056E+00
24 0.27182E+02 0.45645E+00 0.38099E-02 0.17732E+01 0.39506E+01 0.45274E-01
25 0.27531E+02 0.74219E+02 0.61949E+00 0.80649E+02 0.87345E+02 0.10010E+01
26 0.28520E+02 0.22045E+02 0.18400E+00 0.99915E-02 0.23962E+02 0.27461E+00
27 0.29205E+02 0.15591E+01 0.13014E-01 0.40383E+01 0.76756E+01 0.87964E-01
28 0.29311E+02 0.56079E+02 0.46808E+00 0.15419E+01 0.99441E+02 0.11396E+01
29 0.30040E+02 0.42202E+03 0.35225E+01 0.32876E+03 0.24713E+03 0.28322E+01
30 0.30167E+02 0.15056E+02 0.12567E+00 0.11580E+02 0.85593E+01 0.98092E-01
31 0.31258E+02 0.77068E+03 0.64327E+01 0.43419E+03 0.19359E+03 0.22186E+01
32 0.32120E+02 0.27797E+03 0.23201E+01 0.14986E+01 0.36560E+03 0.41899E+01
33 0.32290E+02 0.78402E+01 0.65441E-01 0.99158E+00 0.22959E+02 0.26312E+00
34 0.33043E+02 0.38374E+03 0.32030E+01 0.50905E-02 0.38935E+03 0.44620E+01
35 0.33707E+02 0.24152E+02 0.20159E+00 0.37537E+02 0.53861E+02 0.61726E+00
36 0.34679E+02 0.20283E+00 0.16930E-02 0.75805E+00 0.16665E+01 0.19099E-01
37 0.35588E+02 0.71714E+02 0.59859E+00 0.37515E+01 0.21111E+02 0.24194E+00
38 0.36219E+02 0.10796E+04 0.90108E+01 0.64775E+03 0.32564E+03 0.37319E+01
39 0.36414E+02 0.24699E+01 0.20616E-01 0.66358E+00 0.10245E+02 0.11741E+00
40 0.36842E+02 0.11731E+03 0.97915E+00 0.48513E+02 0.96064E+01 0.11009E+00
41 0.37393E+02 0.88986E+02 0.74275E+00 0.34277E+02 0.51802E+01 0.59367E-01
42 0.37620E+02 0.23237E+02 0.19395E+00 0.21818E+01 0.34832E+01 0.39918E-01
43 0.37677E+02 0.16580E+01 0.13839E-01 0.64111E+00 0.98435E-01 0.11281E-02
44 0.38063E+02 0.30028E+03 0.25064E+01 0.37079E+01 0.44859E+03 0.51409E+01
45 0.38309E+02 0.13478E+03 0.11250E+01 0.23504E+01 0.21537E+03 0.24682E+01
46 0.39121E+02 0.14031E+03 0.11711E+01 0.67799E+02 0.21371E+02 0.24492E+00
47 0.39593E+02 0.89880E+02 0.75021E+00 0.15929E+03 0.24843E+03 0.28471E+01
48 0.40165E+02 0.15722E+02 0.13123E+00 0.17319E+01 0.43522E+02 0.49878E+00
49 0.40301E+02 0.20544E+00 0.17148E-02 0.85479E+00 0.53008E+01 0.60749E-01
50 0.40888E+02 0.11863E+03 0.99020E+00 0.46471E+02 0.75195E+01 0.86175E-01
51 0.41278E+02 0.73059E+02 0.60981E+00 0.28853E+02 0.37212E+03 0.42646E+01
52 0.42287E+02 0.14886E+03 0.12425E+01 0.32855E+02 0.54298E+00 0.62226E-02
53 0.42519E+02 0.28046E+01 0.23410E-01 0.36636E+02 0.10880E+03 0.12469E+01
54 0.42898E+02 0.29552E+01 0.24667E-01 0.19184E+02 0.49575E+02 0.56814E+00
55 0.43364E+02 0.18463E+03 0.15411E+01 0.16739E+03 0.15101E+03 0.17306E+01
56 0.44082E+02 0.22513E+01 0.18791E-01 0.23481E+02 0.67092E+02 0.76890E+00
57 0.44562E+02 0.11253E+03 0.93923E+00 0.26921E+01 0.53674E+02 0.61512E+00
58 0.44698E+02 0.38055E+01 0.31763E-01 0.30012E+01 0.22923E+01 0.26270E-01
59 0.44882E+02 0.19191E+02 0.16018E+00 0.17287E+02 0.15483E+02 0.17743E+00
60 0.45689E+02 0.16111E+00 0.13448E-02 0.11889E+03 0.49323E+03 0.56525E+01
61 0.45849E+02 0.18643E+01 0.15561E-01 0.23798E+02 0.12370E+03 0.14177E+01
62 0.46062E+02 0.25821E+01 0.21552E-01 0.14930E+02 0.87137E+02 0.99862E+00
63 0.47051E+02 0.52186E+02 0.43558E+00 0.80128E+01 0.16603E+03 0.19028E+01
64 0.47434E+02 0.44184E+00 0.36880E-02 0.21305E+02 0.73389E+02 0.84105E+00
65 0.47609E+02 0.13942E+02 0.11637E+00 0.25534E+02 0.40607E+02 0.46536E+00
66 0.47851E+02 0.18237E+01 0.15222E-01 0.38714E+01 0.66808E+01 0.76564E-01
67 0.49249E+02 0.11068E+02 0.92380E-01 0.91477E+00 0.27454E+02 0.31463E+00
68 0.49345E+02 0.19097E+02 0.15939E+00 0.92000E+01 0.28776E+01 0.32978E-01
69 0.50002E+02 0.74994E+01 0.62596E-01 0.47743E+02 0.12278E+03 0.14071E+01
70 0.51670E+02 0.14946E+02 0.12475E+00 0.18317E+02 0.15439E+03 0.17694E+01
71 0.52631E+02 0.11993E+00 0.10010E-02 0.11259E+00 0.10548E+00 0.12088E-02
72 0.53359E+02 0.45907E+02 0.38318E+00 0.77303E+02 0.11683E+03 0.13389E+01
73 0.54022E+02 0.18226E+01 0.15213E-01 0.24196E+00 0.13415E+00 0.15374E-02
74 0.54733E+02 0.10983E-01 0.91669E-04 0.49781E+00 0.17065E+01 0.19557E-01
75 0.54839E+02 0.14145E+01 0.11807E-01 0.56706E+01 0.12768E+02 0.14633E+00
76 0.55304E+02 0.15644E+01 0.13058E-01 0.12118E+02 0.32620E+02 0.37384E+00
77 0.55643E+02 0.14909E+02 0.12444E+00 0.27572E+02 0.20630E+03 0.23642E+01
78 0.55907E+02 0.12783E+01 0.10670E-01 0.69653E+01 0.17204E+02 0.19716E+00
79 0.56227E+02 0.22216E+00 0.18543E-02 0.11431E+02 0.39574E+02 0.45352E+00
80 0.57088E+02 0.98621E+00 0.82317E-02 0.20360E+01 0.14798E+02 0.16959E+00
81 0.57376E+02 0.25514E+01 0.21296E-01 0.10028E+01 0.12961E+02 0.14854E+00
82 0.57918E+02 0.12539E+01 0.10466E-01 0.72453E+01 0.42291E+02 0.48467E+00
83 0.60574E+02 0.35581E+01 0.29699E-01 0.40761E+01 0.46293E+01 0.53053E-01
84 0.62217E+02 0.17523E+01 0.14626E-01 0.57877E+00 0.80956E+01 0.92778E-01
85 0.62937E+02 0.55953E+00 0.46703E-02 0.20991E+01 0.46211E+01 0.52959E-01
86 0.64088E+02 0.58865E+01 0.49134E-01 0.33925E+00 0.12896E+02 0.14779E+00
87 0.64946E+02 0.71390E-03 0.59588E-05 0.87721E+01 0.35406E+02 0.40576E+00
```

```
88 0.65055E+02 0.16670E+01 0.13914E-01 0.30082E+01 0.47423E+01 0.54348E-01
89 0.66061E+02 0.39263E+01 0.32772E-01 0.74594E+01 0.12116E+02 0.13886E+00
90 0.66909E+02 0.14988E+01 0.12511E-01 0.12011E+01 0.11670E+02 0.13375E+00
91 0.67214E+02 0.27440E+00 0.22904E-02 0.41445E+01 0.21118E+02 0.24202E+00
92 0.68139E+02 0.12022E+01 0.10034E-01 0.52326E+01 0.32165E+02 0.36862E+00
93 0.68859E+02 0.13657E-01 0.11399E-03 0.47533E-02 0.64899E-01 0.74376E-03
94 0.70434E+02 0.75054E+00 0.62646E-02 0.84891E+00 0.73390E+01 0.84107E-01
95 0.70797E+02 0.18575E+01 0.15505E-01 0.31002E-02 0.21735E+01 0.24909E-01
96 0.75336E+02 0.59565E-01 0.49717E-03 0.12236E+01 0.38742E+01 0.44400E-01
97 0.76913E+02 0.13950E+00 0.11644E-02 0.15778E+01 0.45741E+01 0.52421E-01
98 0.77520E+02 0.43121E+00 0.35992E-02 0.10207E+00 0.31281E-03 0.35849E-05
99 0.79277E+02 0.24285E+00 0.20270E-02 0.64722E+00 0.44176E+01 0.50626E-01

SUM RULES FOR IS:
M(-1) =0.764581E+03
M(0) =0.119806E+05
M(1) =0.278969E+06
M(3) =0.284426E+09
M(1) D.C. =0.280433E+06
% EXHAU. =0.994778E+02%

SUM RULES FOR IV:
M(-1) =0.330963E+03
M(0) =0.872580E+04
M(1) =0.290937E+06
M(3) =0.483832E+09
M(1) D.C. =0.295711E+06
% EXHAU. =0.983856E+02%

CONSTRAINED, CENTROID, SCALING ENERGIES:
SQRT[M(1)/M(-1)] (IS) =0.191014E+02
M(1)/M(0) (IS) =0.232850E+02
SQRT[M(3)/M(1)] (IS) =0.319306E+02

SQRT[M(1)/M(-1)] (IV) =0.296490E+02
M(1)/M(0) (IV) =0.333422E+02
SQRT[M(3)/M(1)] (IV) =0.407801E+02
```

References

[1] M.N. Harakeh, A.M. Van Der Woude, Giant Resonances: Fundamental High-Frequency Modes of Nuclear Excitations, Oxford University Press, Oxford, 2001.
[2] D. Vautherin, D.M. Brink, Phys. Rev. C 5 (1972) 626.
[3] S. Krewald, V. Klemt, J. Speth, A. Faessler, Nuclear Phys. A 281 (1977) 166.
[4] G.F. Bertsch, S.F. Tsai, Phys. Rep. 18 (1975) 125.
[5] S. Shlomo, G.F. Bertsch, Nuclear Phys. A 243 (1975) 507.
[6] K.F. Liu, N. Van Giai, Phys. Lett. B 65 (1976) 23.
[7] S. Fracasso, G. Colò, Phys. Rev. C 72 (2005) 064310.
[8] T. Sil, S. Shlomo, B.K. Agrawal, P.-G. Reinhard, Phys. Rev. C 73 (2006) 034316.
[9] G. Colò, P.F. Bortignon, S. Fracasso, N. Van Giai, Nuclear Phys. A 788 (2007) 137c.
[10] T. Nakatsukasa, T. Inakura, K. Yabana, Phys. Rev. C 76 (2007) 024318.
[11] J. Daoutidis, P. Ring, Phys. Rev. C 80 (2009) 024309.
[12] E. Chabanat, P. Bonche, P. Haensel, J. Meyer, R. Schaeffer, Nuclear Phys. A 635 (1998) 231; Nuclear Phys. A 643 (1998) 441.
[13] M. Beiner, H. Flocard, N. Van Giai, P. Quentin, Nuclear Phys. A 238 (1975) 29.
[14] T.H.R. Skyrme, Phil. Mag. 1 (1956) 1043.
[15] T.H.R. Skyrme, Nuclear Phys. 9 (1959) 615.
[16] S. Fracasso, G. Colò, Phys. Rev. C 76 (2007) 044307.
[17] J.C. Slater, Phys. Rev. 81 (1951) 85.
[18] C. Titin-Schnaider, Ph. Quentin, Phys. Lett. B49 (1974) 397.
[19] P. Ring, P. Schuck, The Nuclear Many-Body Problem, Springer-Verlag, New York, 1980.
[20] D.J. Rowe, Nuclear Collective Motion, Methuen and Co. Ltd., London, 1980.
[21] N. Ullah, D.J. Rowe, Nuclear Phys. A163 (1971) 257.
[22] J.M. Eisenberg, W. Greiner, Nuclear Theory. Vol. II. Excitation Mechanisms of the Nucleus, North-Holland, Amsterdam, 1988.
[23] A. Bohr, B.R. Mottelson, Nuclear Structure, Vol. I, W.A. Benjamin, Reading, 1969.
[24] D.J. Thouless, Nuclear Phys. 22 (1961) 78.
[25] N. Van Giai, H. Sagawa, Nuclear Phys. A371 (1981) 1.
[26] N. Van Giai, H. Sagawa, Phys. Lett. B106 (1981) 379.
[27] J. Bartel, Ph. Quentin, M. Brack, C. Guet, H.-B. Håkansson, Nuclear Phys. A386 (1982) 79.
[28] J. Dobaczewski, H. Flocard, J. Treiner, Nuclear Phys. A 422 (1984) 103.
[29] P.-G. Reinhard, H. Flocard, Nuclear Phys. A584 (1995) 467.
[30] P.-G. Reinhard, D.J. Dean, W. Nazarewicz, J. Dobaczewski, J.A. Maruhn, M.R. Strayer, Phys. Rev. C60 (1999) 014316.
[31] L.G. Cao, U. Lombardo, C.W. Shen, N. Van Giai, Phys. Rev. C73 (2006) 014313.
[32] J. Dobaczewski, J. Dudek, Phys. Rev. C52 (1995) 1827. (See also the erratum: Phys. Rev. C55, 3177 (1997)).